Enhancing Motor Cortex Excitability in Mice Through Optogenetic Intermittent Theta Burst Stimulation

Shafik Algharbi

Thesis submitted to the University of Ottawa
in partial Fulfillment of the requirements for the
Master of Science in Neuroscience

Department of Cellular and Molecular Medicine
Faculty of Medicine
University of Ottawa

Abstract

The motor cortex (MCX) is integral to voluntary movement, sending signals from the brain to spinal motoneurons through the corticospinal tract. Enhancing MCX offers the potential for improving motor function in healthy individuals and aiding recovery post-stroke. Intermittent theta burst stimulation (iTBS) has shown promise in increasing MCX excitability in clinical settings, but its effects are often short-lived and lack spatiotemporal precision. Additionally, the use of invasive tools in animal models to study iTBS presents further challenges to its development. To overcome these limitations, this thesis will use a noninvasive approach that combines transcranial optogenetics with iTBS (opto-iTBS), offering high spatiotemporal precision and aiming to achieve more sustained enhancements in cortical excitability.

We hypothesized that opto-iTBS significantly increases cortical excitability and motor output in naïve mice. Specifically, we designed four noninvasive metrics, including tracking evoked forelimb movement, recording blood flow and epidural EEG signal, and using light-based motor mapping to track changes in the MCX pre- and post-opto-iTBS.

We established an iTBS protocol in mice using transcranial optogenetic stimulation. Using blue light stimulation in ketamine/xylazine anesthetized Thy1-ChR2 mice, we measured the time course of enhanced cortical excitability based on the amplitude of evoked forelimb movements and EEG recordings from the MCX. Stimulation was performed through a transcranial chronic window that provides optical access to the MCX in both hemispheres, thus allowing repeated assessments of iTBS effects. Laser Doppler imaging recorded blue light-evoked hemodynamic

changes in the MCX during iTBS. Epidural EEG electrodes collected blue light evoked signals from around the stimulation region.

Our findings demonstrate that opto-iTBS significantly increases the optogenetically evoked contralateral forelimb movement amplitude for at least 85 minutes post-stimulation and expands the size and activation threshold of the motor map for a minimum of 10 minutes. Additionally, a significant increase in blood flow at the stimulation site in the MCX was observed during opto-iTBS induction.

Our noninvasive optogenetic stimulation approach enables longitudinal experiments that allow multi-target assessment, control of stimulation parameters, and within-subject measures of treatment effects. By elucidating optimal parameters and targets for iTBS, this research may identify therapeutic interventions to improve function following MCX stroke.

Table of Contents

List of Figures

List of Tables

List of Supplemental Figures

Acknowledgment

I dedicate this thesis to my late father, Nabil Algharbi, who was a loving father, a successful Engineer, and a genuine, intelligent, and caring man. His life lessons and words of wisdom continue to guide me through every step of my journey. His dedication to excellence and passion for learning inspired my academic pursuits. I also dedicate this to my mother, Maya Sneig, whose boundless love and unwavering support carried me through our shared challenges. Her remarkable strength and personal success motivated me to persist in my studies, while her nurturing spirit and endless encouragement kept me focused and determined. Finally, I dedicate this to my better half, Jassica Adamo, who has been my pillar of strength through every triumph and challenge. Her unconditional love, understanding, and continuous encouragement to pursue my dreams have been instrumental in my academic journey. I am forever grateful to these remarkable individuals, along with my extended family and friends, who have supported me in countless ways throughout this journey.

I express my deepest gratitude to my supervisor, Dr. Greg Silasi, who has guided me since my fourth year of undergraduate studies. His mentorship extended beyond the laboratory, fostering both my scientific growth and professional development. Together, we successfully completed this project and presented our findings at the Society for Neuroscience meeting, marking a significant milestone in my research career. Dr. Silasi's expertise, patience, and dedication to scientific excellence have profoundly shaped my understanding of Neuroscience and research methodology.

I am grateful to my fellow lab members, past and present, who created an enriching research environment filled with collaboration and support. Their valuable insights and constructive feedback significantly enhanced my project. Special thanks to Zachary Eckert and Eilia Dizgah for their thoughtful discussions and expert guidance in motor mapping during my early training stages. I am particularly indebted to Arvin Zaker for his exceptional assistance with R analysis scripts and the LDI project. I extend special recognition to Irina Morozov, our outstanding lab engineer, whose technical expertise and innovative contributions to the automated ketamine pump project were invaluable.

I sincerely thank my thesis advisory committee members, Dr. Béïque and Dr. Tremblay, for their insightful guidance and constructive feedback that strengthened my research. I acknowledge the dedicated staff of the animal care facility for their essential support in surgery and animal housing. I am grateful to the Faculty of Medicine and the Department of Neuroscience, particularly to Dr. Lagace, whose leadership has been exceptional. Her unique combination of intellectual rigor and nurturing approach creates an ideal environment for student success. Her encouragement and support have been vital throughout my graduate studies.

Finally, I gratefully acknowledge the Natural Science and Engineering Research Council (NSERC) for their financial support, which made this research possible.

1.0 Introduction

1.1 MCX

The skilled movements we perform in our everyday lives are controlled by descending projections from the brain that terminate at our muscles [1,2]. Specifically, neurons in the motor cortex (MCX) project to the spinal cord via the corticospinal tract, forming synapses primarily with interneurons and, in some cases, directly with motor neurons in the ventral horn. These motor neurons then innervate skeletal muscles, enabling voluntary movement [3,4]. The MCX generates voluntary movement by integrating sensory input and coordinating motor output to produce precise movements [5,6]. This is evidenced by studies showing that MCX neurons modulate their firing rates to optimize force production and timing of muscle activation patterns during learned motor tasks [7–9].

1.1.1 MCX Projections

The MCX's control over voluntary movement is organized hierarchically through its primary (M1) and secondary motor areas (M2) [1,3]. Layer V of M1 contains specialized Betz cells, which form direct corticospinal projections crucial for precise movement execution. M2 areas, including the preMCX, contribute to movement control through both direct corticospinal projections and modulatory circuits that help coordinate complex movements and integrate sensory feedback[10]. This hierarchical organization enables immediate motor execution through direct corticospinal pathways from both regions while also supporting higher-order functions such as movement planning and adaptation through additional processing circuits.

1.1.2 MCX Plasticity and Motor Learning

The MCX coordinates voluntary movement through precisely timed activation of specific muscle groups[1,3]. Independent of this basic control function, the MCX also exhibits plasticity mechanisms that support motor learning and skill acquisition. Studies have shown that repeated practice of motor tasks can lead to structural and functional changes within the MCX, resulting in an expanded representation of the trained muscles and improved motor output [7,11]. This adaptability, known as plasticity, enables us to refine motor skills and adjust our movements based on sensory feedback, allowing smooth and coordinated interactions with our environment MCX [12–16]. These findings have significantly advanced our understanding of the neural mechanisms underlying motor skill acquisition and refinement.

1.1.3 MCX Injury and Motor Deficits

Damage to the MCX can disrupt descending motor pathways and lead to significant impairments in movement control [10,17,18]. Such injuries often result in weakness or loss of control in the affected limbs and diminished ability to perform precise, coordinated movements [19]. The consequences of MCX damage are particularly evident in conditions such as stroke, where disruption of cortical function can impair communication with the spinal cord and muscles, leading to deficits in motor control and requiring rehabilitation efforts to restore functionality [18,20–22]. Understanding these injury mechanisms and their consequences is crucial for developing effective therapeutic strategies.

1.2 Theta Burst and MCX Plasticity

The MCX may exhibit plasticity through changes in neural activity patterns, including those induced by external interventions like using a form of repetitive transcranial magnetic stimulation (rTMS), known as theta burst stimulation (TBS) [23–26]. However, the effects on synaptic plasticity reported in these experiments were often weak, highly variable between individuals, and short-lived [15,16]. TBS is a patterned stimulation protocol involving high frequency (50–200 Hz) bursts spaced at theta rhythm (3–8 Hz) [27]. Understanding how TBS influences MCX function may be essential for developing effective neuromodulation approaches.

1.2.1 Theta Burst Stimulation in Experimental Models

TBS has been reported to induce plasticity in other brain regions [28–37]. Early studies examining TBS in hippocampal brain slices revealed its potentiating effects on synaptic strength. Larson and Lynch (1986) were among the first to demonstrate that delivering bursts of high-frequency pulses at theta intervals reliably induced long-term potentiation (LTP) in rats hippocampal neurons [36]. This foundational work highlighted the critical role of theta-patterned stimulation in driving synaptic modifications, laying the groundwork for subsequent applications of TBS in other brain regions. In the MCX, it has been demonstrated that TBS reliably induced LTP in horizontal connections of layer II/III in rat motor cortex slices [37]. This LTP was contingent on a transient reduction of local inhibition, achieved using a $GABA_A$ receptor antagonist. Results showed a sustained increase in synaptic efficacy, with field potential amplitudes increasing by 24–34% after TBS application, providing evidence that TBS may induce plasticity in motor cortical circuits.

On the gene expression side, TBS in the rat MCX altered protein expression related to neurotransmitter release, such as GAD65 and VGLUT1 [38]. These molecular adaptations are consistent with plasticity mechanisms and suggest that patterned stimulation at theta frequencies can induce synaptic changes in motor circuits.

Moreover, cortical electrical stimulation combined with TBS in anesthetized rats demonstrated robust changes in cortical excitability and motor output [39]. Theta-patterned stimulation could reliably modify motor responses, suggesting its potential for studying motor plasticity mechanisms. Similarly, intracortical TBS could entrain neural oscillations at the stimulation site and connected brain regions, indicating its broader effects on motor networks [40].

More recently, focused ultrasound theta burst stimulation as a noninvasive alternative was used, showing that it could enhance motor output similar to electrical stimulation [41]. This parallel finding across different stimulation methods reinforces the fundamental importance of TBS in motor plasticity.

1.2.2 Alternative Stimulation Frequencies

While theta rhythms stimulation affects motor plasticity [42,43], other stimulation frequencies have also been investigated. For instance, gamma frequency stimulation (30-100 Hz) has shown distinct effects on motor function [44–47]. It was shown that gamma stimulation produced more task-specific improvements in motor performance compared to theta stimulation [47]. However, these effects were often limited to specific movement patterns and did not generalize as broadly as theta-based protocols.

Moreover, combining different stimulation frequencies showed that theta-gamma coupling could enhance plasticity beyond what either frequency achieved alone [48]. This finding suggests that while different brain rhythms serve distinct functions, their interaction may be important for optimal motor learning and adaptation.

1.2.3 Short-term Motor Plasticity

The MCX shows rapid adaptability through various forms of short-term plasticity [49,50]. These changes can occur within minutes of targeted stimulation and may last for hours, providing a window to study immediate adaptive responses [51]. In both animal models and human studies, brief periods of rhythmic stimulation can temporarily enhance or suppress motor output, depending on the stimulation pattern used [15,52–54].

Forelimb representations were mapped in mice using high-frequency stimulation, revealing how brief interventions could modify movement patterns [55]. Their work demonstrated that even short periods of stimulation could reorganize motor outputs, suggesting a dynamic relationship between stimulation patterns and movement control. These findings align with human studies showing rapid motor adaptations following brief periods of training or stimulation.

The duration of these short-term changes varies based on stimulation parameters. It was found that brief periods of theta burst stimulation could influence MCX excitability for up to an hour after stimulation, with corresponding changes in movement control [56,57]. These temporary modifications provide insight into how the MCX rapidly adjusts its output based on incoming signals, forming the basis for longer-term adaptations that support motor learning.

1.2.4 Translation to Clinical Applications

While animal studies have established the fundamental principles of MCX plasticity and rhythmic stimulation, translating these findings into human applications may require noninvasive approaches [58]. The need to modulate MCX function without surgical intervention has driven the development of various noninvasive brain stimulation techniques. These methods aim to harness the plasticity principles discovered in experimental models while maintaining safety and accessibility for clinical use [58].

1.3 Noninvasive Brain Stimulation

NBS refers to a range of techniques used to modulate brain activity without requiring invasive procedures [59–61]. Transcranial Magnetic Stimulation (TMS) is widely recognized for its effectiveness in targeting specific brain regions [61]. TMS generates magnetic fields that induce electric currents in the brain, transiently activating or inhibiting local neuronal circuits [19,62–67]. TMS can trigger lasting changes in synaptic transmission through repeated application, making it valuable for both research and clinical applications, especially in treating neurological conditions and promoting motor recovery after injuries like stroke [68,69].

TMS can be applied as either single pulses or repetitive stimulation protocols. Single TMS pulses, delivered by positioning a coil over the scalp, generate brief electric fields that trigger action potentials in underlying neural tissue, probing cortical function and mapping brain regions like MCX[19,68]. In contrast, rTMS involves delivering multiple pulses in specific patterns, which can induce lasting changes in synaptic transmission. This ability of rTMS to modify neural circuits has shown promise in therapeutic applications, particularly in stroke rehabilitation,

where carefully designed stimulation protocols can promote motor recovery by strengthening specific corticospinal pathways and their connections [70,71].

1.3.1 Transcranial Direct Current Stimulation

Another prominent NBS technique is transcranial direct current stimulation (tDCS), which delivers weak electrical currents through electrodes placed on the scalp [61,72,73]. Unlike TMS's focused magnetic pulses, tDCS applies a constant, low-intensity electrical current to modulate neural activity, though the mechanism of action remains under debate. Early interpretations suggested that anodal stimulation typically increased cortical excitability while cathodal stimulation decreased it [73,74]; however, more recent findings indicate that such polarity-specific effects are inconsistent across individuals or brain states. Current evidence shows that a large portion of the applied current is attenuated by the scalp and skull, with less than 25% reaching the brain. Fields strong enough to directly influence spiking or subthreshold activity require intracranial electric field gradients of at least ~1 mV/mm, values that conventional tDCS rarely achieves. Effects observed at standard intensities may instead reflect indirect mechanisms such as entrainment of neural oscillations, modulation of peripheral nerves, or state-dependent biasing of ongoing network activity [75,76]. While tDCS remains appealing due to its low cost, portability, and ease of use, its diffuse current spread, unclear physiological mechanisms, and variable individual responses limit its utility for applications requiring precise spatial and temporal control of neural activity.

1.3.2 Intermittent Theta Burst Stimulation

Specific protocols have been developed within the rTMS framework to achieve different modulatory effects. Intermittent Theta Burst Stimulation (iTBS) induces cortical excitation through a carefully structured delivery pattern [15,16]. iTBS involves delivering bursts of three magnetic pulses at 50 Hz, repeated every 200 ms (5 Hz) at a theta rhythm (4 – 8 Hz), which aligns with natural brain rhythms associated with learning and plasticity [15,77–80]. Each iTBS session typically consists of 600 pulses, delivered over a brief period, making it an efficient tool for inducing excitatory changes in the MCX [53]. This protocol has been shown to produce long-term potentiation (LTP)-like effects, a mechanism associated with neuroplasticity and learning [25,81]. Studies indicate that iTBS can improve motor function in stroke patients by enhancing the excitability of motor pathways, potentially leading to better motor outcomes [54,82].

1.3.3 Continuous Theta Burst Stimulation

In contrast to iTBS, Continuous Theta Burst Stimulation (cTBS) is generally considered an inhibitory protocol within the rTMS family [83,84]. In cTBS, the same bursts of pulses are delivered continuously over a short period, leading to long-term depression (LTD)- like effects that reduce cortical excitability [83]. However, the effects of cTBS appear to be region-specific. While it tends to suppress motor cortical excitability, studies have shown that cTBS can induce facilitatory effects in other cortical regions, such as the prefrontal cortex and cerebellum. This bidirectional response pattern likely reflects differences in local circuit organization and baseline activity states across brain regions [15,85]. The applications of cTBS thus require careful consideration of the targeted brain region and individual physiological factors, as its effects can vary based on stimulation parameters, brain state, and individual neurophysiological characteristics [86].

1.4 Clinical and Preclinical Challenges

Despite these promising approaches, the clinical application of TMS faces significant challenges, particularly in protocols like iTBS and cTBS, due to the lack of spatiotemporal precision needed for individualized treatment responses [22]. While TMS can effectively modulate cortical excitability, individual variability in brain anatomy and lesion characteristics, especially in stroke patients, makes it challenging to achieve consistent therapeutic outcomes [87]. Clinical settings cannot often deliver precisely targeted stimulation, limiting the translation of TMS benefits observed in controlled research environments to broader patient populations.

Clinical trials investigating noninvasive brain stimulation have reported inconsistent effects of techniques such as iTBS on the MCX [15,57,58,88], largely due to the limitations outlined earlier in this thesis. To address these gaps, a more fundamental understanding of how the MCX responds to stimulation protocols like iTBS is needed. Rodent models provide a powerful tool for this inquiry, allowing control over variables such as neuronal population targeting and brain region specificity while enabling advanced imaging and stimulation techniques [39,53,54,89,90]. These advantages offer deeper insights into the motor system's response to high-frequency stimulation; however, rodent models also present their own set of limitations.

1.4.1 Invasive Stimulation Techniques in Rodents

The investigation of clinical challenges has led researchers to employ TMS and more invasive techniques in preclinical studies [58]. However, traditional invasive methods like intracortical microstimulation (ICMS) present significant methodological limitations, particularly for longitudinal investigations [91–93]. ICMS requires surgical implantation of microelectrodes directly into the cortical tissue, inevitably compromising the structural and functional integrity of the

surrounding neural tissue. This invasive approach introduces confounding variables through mechanical trauma, local inflammatory responses, and microlesions in the neural tissue surrounding the implantation site [94,95]. These tissue reactions can persist throughout the experimental timeline, potentially biasing results with effects not directly attributable to the intended stimulation parameters.

1.4.2 Anesthesia Protocol Variability in Rodents

Another significant challenge across these preclinical studies has been the lack of standardization in anesthesia protocols [58,96,97]. While Ketamine and Xylazine are commonly used to stabilize rodents during experiments, the administration methods vary significantly between research groups [96–99]. Different protocols for initial dosing and maintenance during experiments may introduce potential variability in results. Additionally, there has been no standardized protocol for determining if an animal maintains the same anesthesia state throughout the experiment. This inconsistency in anesthesia levels can create significant variability in recorded responses during experiments, making it difficult to compare results across studies or even within the same experimental session.

1.4.3 Intracortical Optogenetics

Even more advanced techniques like intracortical optogenetics, while offering precise control over specific brain cells through light stimulation, still face similar invasiveness challenges. The required surgical insertion of optical fibers through the skull results in tissue damage that can confound experimental results [39,53]. Though optogenetics provides better targeting accuracy than electrical stimulation methods, the physical presence of inserted devices and associated tissue

disruption makes it difficult to isolate the effects of stimulation from those of the surgical intervention.

The technique involves introducing light-sensitive proteins into target neurons; typically, Channelrhodopsin-2 (ChR2) is used, enabling activation with exceptional temporal and spatial precision [100–104]. In previous studies, ChR2(H134R) was delivered via a lentiviral vector under the CaMKIIα promoter to selectively target excitatory glutamatergic neurons. The virus was packaged using a second-generation lentiviral system and injected intracranially to achieve expression in the motor cortex. They used intracranial optogenetics to modulate the excitability of the MCX in rodents. One of those studies investigated the effects of intracranial optogenetic theta burst stimulation on motor excitability in rats, finding that this type of stimulation could modulate motor excitability in a frequency-dependent manner [53]. Another study used intracranial optogenetic stimulation in rats to investigate its potential for modulating motor plasticity. It discovered that repeated stimulation could produce persistent strengthening of corticospinal motor output and durable spinal cord structural changes [39]. A more recent investigation examined the effects of repeated MCX theta-burst stimulation on corticospinal motor output and spinal cord structural changes in rats [39,54]. Specifically, both studies suggest that this stimulation can produce persistent strengthening of corticospinal motor output and durable spinal cord structural changes, with potential implications for developing post-stroke therapeutic interventions.

Further complicating these investigations is the reliance on invasive recording techniques to monitor changes in MCX function. Local field potentials (LFPs) require electrode insertion near the stimulation site, while electromyography (EMG) necessitates electrode placement directly into muscles to measure responses [105–108]. These methods introduce additional tissue damage and

inflammation, potentially altering the phenomena they aim to study. This creates a fundamental challenge in animal research: obtaining reliable, unbiased data on neuroplasticity without inflicting injury that could change or limit the scope of the findings.

1.5 An All-In-One Noninvasive Approach to Bridge the Gap

The challenges in both clinical and preclinical settings highlight critical gaps and limitations in NBS development [58]. Clinically, while TMS offers noninvasive stimulation, it lacks cellular specificity and faces challenges in delivering consistent, precisely targeted stimulation [58,109]. Preclinically, traditional methods like ICMS and intracranial optogenetics, though providing valuable insights, are limited by tissue damage and inflammatory responses that confound results [53,110]. The reliance on invasive recording techniques to monitor changes in MCX function further complicates these investigations [111,112]. Furthermore, the variability in anesthesia protocols across studies has introduced additional inconsistencies in experimental outcomes [96,97,99]. These combined challenges underscore the need for a comprehensive approach to provide precise stimulation while maintaining tissue integrity and experimental standardization.

1.5.1 Transcranial Optogenetics

This thesis aims to address these challenges by utilizing the development of transcranial optogenetics, which offers new possibilities for stimulating the brain in a precise and noninvasive way. This technique delivers light through an intact skull, preserving brain tissue integrity and enabling longitudinal experiments. Within this noninvasive framework, several complementary metrics like recording evoked forelimb movement, epidural electroencephalogram (EEG) and blood flow, and light-based motor mapping (LBMM) can be employed to assess MCX changes without causing more damage. High-frame-rate video

recording provides a noninvasive method to capture evoked forelimb movements generated by optogenetic stimulation of MCX. Epidural EEG recordings provide information about the timing and amplitude of neural population responses to optogenetic stimulation, allowing us to measure how different stimulation patterns affect cortical activation and connectivity. By recording these electrical signals from electrodes placed in the epidural space, we can directly measure the neural response to optogenetic stimulation without penetrating brain tissue, providing a noninvasive insight into immediate circuit activation changes.

Additionally, laser Doppler imaging (LDI) through chronic cranial windows enables noninvasive monitoring of blood flow changes during optogenetic stimulation. These measurements reveal how neural activation patterns influence local blood flow, providing a secondary marker of successful stimulation and helping verify the spatial extent of cortical activation. By measuring neurovascular coupling - the relationship between neural activity and blood flow - we can better understand how different stimulation parameters affect both neural circuits and their metabolic demands. LBMM techniques complement these measurements by comprehensively assessing evoked forelimb response changes across both MCX hemispheres at different stimulation points. This mapping approach allows us to track how stimulation-induced plasticity may alter the size and organization of motor representations in the MCX.

These noninvasive measurement approaches integrate seamlessly with a standardized anesthesia protocol, where all mice receive weight-adjusted doses of Ketamine and Xylazine, with maintenance provided through an automated ketamine infusion pump. This unified approach to anesthesia management ensures consistent physiological states across experiments. Integrating iTBS and cTBS protocols using transcranial optogenetics, known as opto-iTBS and opto-cTBS,

provides a noninvasive means for precisely stimulating specific brain regions while maintaining these standardized conditions. Together, these advances create a comprehensive platform that addresses the longstanding challenges of precise stimulation and experimental standardization, opening new avenues for understanding MCX plasticity and further developing therapeutic interventions.

2.0 Methods

2.1 Animals

All experimental procedures adhered to the guidelines set by the Canadian Council on Animal Care and received approval from the University of Ottawa Animal Care Committee. The study used male and female Thy1-ChR2-YFP mice (n = 38; 22 male, 16 female; B6.Cg-Tg(Thy1-COP4/EYFP)18Gfng/J; 007612, The Jackson Laboratory) aged between 3 and 12 months. Mice were bred and housed in a controlled environment with a 12-hour light/dark cycle. Subjects were randomly assigned to one of three groups: iTBS (n = 22), Sham (n = 20), or cTBS (n = 6). Each mouse participated in two separate stimulation sessions, spaced at least one week apart to allow for recovery and minimize any potential carryover effects.

2.3 Chronic transcranial window and EEG implant

Transcranial chronic windows were prepared following the method described by Silasi et al. (2016). Briefly, animals were anesthetized with isoflurane (4% for induction and 1.5-2.5% for maintenance in 0.3 L/min O2) and given a subcutaneous injection of meloxicam (5 mg/kg). The scalp was removed from an approximately 8mm diameter area, the skull was cleared of fascia and connective tissue and fitted with a circular glass coverslip (Ted Parker; product #260368, 8 mm ⌀) using clear-drying dental cement (Parkell; product: C&B Metabond, SKU: S380) (Fig. 1B).

To facilitate head fixation, a small setscrew (McMaster-Carr; product #94355A216) was embedded in the Metabond posterior to the cranial window. In order to record EEG during experiments, two stainless steel electrodes were positioned epidurally in each hemisphere

approximately 5 mm lateral to bregma. The electrodes were fabricated from acupuncture needles (Dongbang Acupuncture Needles® DB101 0.25 X 15) that were trimmed to ~5mm once inserted into the skull.

2.4 Optimizing Ketamine/Xylazine Anesthesia Maintenance

During all optogenetic experiments, mice were initially anesthetized with brief (less than 2 min) exposure to isoflurane (4% in 0.3 L/min air). This was followed by an intraperitoneal injection of ketamine (30 mg/kg) and xylazine (3 mg/kg). Mice were then head-fixed over a homeothermic heating pad set to maintain body temperature at 37°C. Optixcare eye lubricant was applied to the cornea to keep it moist during anesthesia. To maintain anesthesia levels during the experiment, ~30 µl of ketamine (10 mg/kg) was administered (every 10 minutes on average) based on response to a toe or tail pinch. However, to eliminate human error in infusion rate and ensure consistent administration of ketamine across all mice, we evaluated 3 different ketamine dosing protocols on the stability of evoked forelimb movements.

All mice received an initial dose of ketamine and xylazine as described above, followed by either no top-ups (group 1), manually injected top-ups (group 2), or an automatic infusion pump of ketamine (10 mg/kg) at a rate of 3 µl per minute using a custom-made infusion pump (group 3) (Fig. 2A-C, respectively). During the experiment, we stimulated a single point in the motor cortex using a range of light powers (0.5 – 8.7mW) and quantified the evoked forelimb movement.

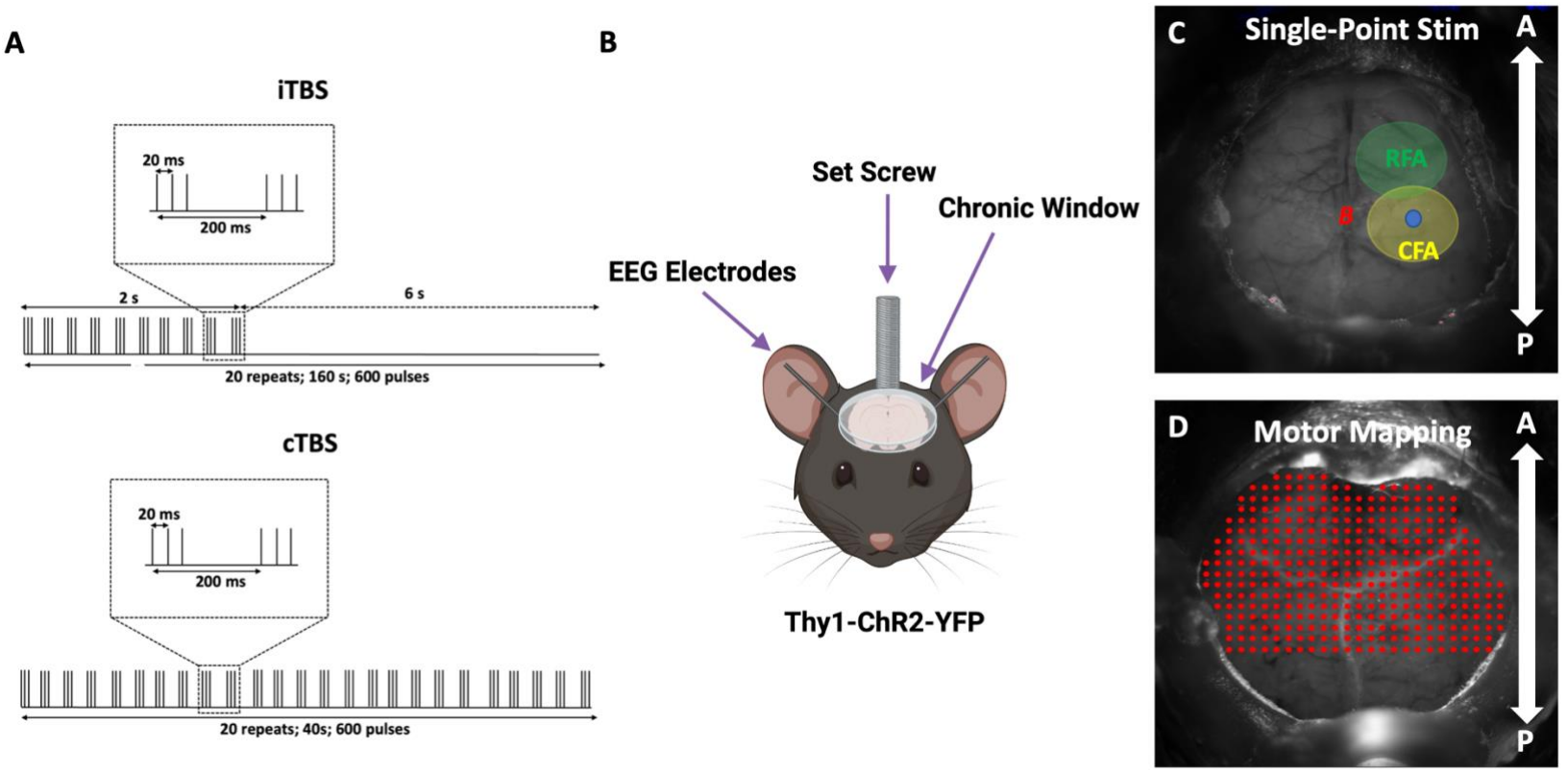

Figure 1. Experimental Setup and Stimulation Protocols. A. Stimulation parameters for iTBS and cTBS: Diagrams depict the light burst frequency, wavelength, and intervals used to apply opto-iTBS and cTBS in the experiment. **B.** Schematic of Thy1-ChR2-YFP mouse with bilateral chronic cranial window, set-screw, and EEG electrodes. **C.** Chronic cranial window axial view: Identifies the single-point stimulation location in the motor cortex (x = 1.5 mm, y = 0.5 mm from bregma). The yellow region highlights the approximate location of the caudal forelimb area (CFA). Meanwhile, the green region highlights the approximate location of the rostral forelimb area (RFA). Red "B" marks the approximate location of bregma. **D.** Light-based motor mapping: Axial view of the chronic cranial window with a grid overlay indicating stimulation points across the cortex during the mapping process. Created with BioRender.com

2.5 Theta Burst Stimulation (TBS)

TBS modulates cortical excitability through bursts of three pulses at 50 Hz, repeated every 200 ms [15,113]. TBS can be administered in two forms: intermittent TBS (iTBS) and continuous TBS (cTBS).

In iTBS, a 2-second train of TBS is repeated every 6 seconds for a total of 160 seconds, resulting in 600 pulses, each lasting for 1 ms (Fig. 1A). In contrast, cTBS delivers a 40-second train of uninterrupted TBS, also totaling 600 pulses (Fig. 1A). In our experiment, these stimulations were administered using 450 nm light with our automated macroscope (LabeoTech).

2.6 Optogenetic probing sessions

A week after the chronic window implantation, mice underwent sessions of transcranial optogenetic stimulation. Blue light was used to elicit forelimb movement from a single point in M1. Mice were head-fixed and positioned securely on an automated macroscope (LabeoTech, LightTrack OiS200 Modular Optical Imaging System), which delivered a 50 µm beam of 450 nm laser light. Forelimb movements were recorded with a high-frame rate camera (900 Hz) focused on the forelimbs. For the high-frequency stimulation, we determined the minimum laser power needed to induce a limb movement, referred to as the resting motor threshold (RMT). This was done by manually stimulating within a 0.5 x 0.5 mm area around the coordinates AP: 0.5 mm, ML: 1.5 mm in the right hemisphere (Fig. 1C). Laser power was measured using a Broad Range Light Meter (Thomas Scientific). The power of a 5 ms laser pulse was increased by 5%-10% increments (starting at 10% of maximum power; ~20 mW) until movement was consistently detected (3 out of 5 stimulations). This setting was used only during optogenetic probing sessions. On average, forelimb movement was detected around ~3 – 5 mW, and iTBS

was delivered at 80% of this power. However, during the ketamine optimization experiment in Figure 2, an ascending range of laser powers (0.5, 2.1, 4.3, 6.5, 8.7 mW) were used to determine optogenetically evoked forelimb response while administering ketamine for anesthesia maintenance throughout the experiment. 0.5 mW represented a low laser power that failed to evoke forelimb movement.

Throughout the experiment, we used a consistent suprathreshold laser intensity (~6.5 mW) to evoke forelimb movements during probing sessions. Our definition of a quantifiable forelimb movement is any evoked forelimb movement size over 1 pixel. After a 10-minute baseline recording period (Fig. 1A), mice are randomized to receive iTBS/cTBS/Sham at an intensity set to 80% of the RMT. We then repeat the probing protocol at five-minute intervals for a total duration of 40-85 minutes. Using custom MATLAB scripts, we quantify the magnitude of evoked forelimb movements at each time point.

2.7 Light-based motor mapping (LBMM)

Mice were subjected to four cortical motor mapping sessions (two baseline and two post-stimulation) Silasi et al. (2013), Zhang et al. (2021) [114,115]. For motor mapping, a grid of stimulation points was superimposed over the cortical surface (300 μm spacing between points, ranging from AP: 3.9 mm, -1.8 mm to ML: 3.3 mm, -3.0 mm) and stimulated in a random order at the RMT, with a 0.5 s interval between stimulations. Stimulation at each site was repeated twice, and responses averaged.

Data analysis was conducted using a custom MATLAB (MathWorks) script to create heat maps of forelimb movement in relation to cortical stimulation sites. Forelimb movements were

included in the analysis if they began between 10-60 ms after stimulation, and movements were tracked until 100 ms post-stimulation. At each stimulation site, evoked forelimb movements were analyzed for maximum movement amplitude, which was defined as the greatest linear displacement of the forelimb during the analysis window. Values smaller than 10% of the largest evoked movement were excluded as such movements are caused by breathing artifacts (Zhang et al. 2021).

2.8 Electroencephalogram (EEG) recording:

EEG signal was recorded from the electrode in the right hemisphere, amplified with a differential amplifier (AM Systems) using a subcutaneous reference electrode in the neck of the mouse. Signals were filtered (high-pass, low-pass, notch), and recorded on a computer through a digitizer. Additionally, a subcutaneous ground electrode is added on the mouse's back.

The effects of light stimulation on EEG signal was assessed by comparing the amplitude, frequency, and duration of stimulation evoked EEG deflections at various time points before and after opto-iTBS . We used an analysis pipeline developed in R (R 4.2.3) language to create and store EEG wave profiles at every time point before and after treatment. This allowed us to investigate changes in electrical activity using peak-to-peak measures at each timepoint to determine the overall amount of evoked activity.

2.9 Laser Doppler Imaging (LDI)

An LDI probe (moorLDI) was used to monitor real-time changes in cerebral blood flow (CBF) at the site of iTBS, cTBS, or Sham stimulation. LDI enables the detection of blood flow by measuring the Doppler shift caused by moving blood cells within the tissue, providing a

continuous measure of flow that reflects relative blood flow changes. Data acquisition was set at 40 Hz, allowing for high temporal resolution during baseline and stimulation sessions, which was essential for detecting potential blood flow changes induced by iTBS.

To enhance data quality, I applied a time constant (TC) filter of 0.1 seconds. This TC filter was chosen to reduce noise in the collected data while minimizing the impact on the temporal resolution necessary for observing meaningful fluctuations in blood flow. The 0.1-second filter allowed for minimal interference with the shape of the flow trace, ensuring a clean, interpretable signal.

In order to synchronize our blood flow recordings with optogenetic stimulation, I integrated a physical shutter into the LDI light path. A Raspberry Pi was programmed to actuate a solenoid as a laser pulse was delivered. The solenoid blocked the LDI laser for 300 milliseconds at the onset of each stimulation. This brief interruption generated a clear artifact in the LDI blood flow recording, precisely marking the beginning of each stimulation session. This approach allowed for accurate alignment between the start of optogenetic stimulation and the LDI trace, thus allowing us to quantify blood flow changes induced by optogenetic stimulation.

2.10 Statistical Analysis

Statistical analysis was conducted using a combination of MATLAB, Python, and R programming languages for data processing, with Prism 10 used for statistical testing and visualization.

2.10.1 Evoked Forelimb Movement Analysis

Evoked forelimb movements of the contralateral (left) forelimb were analyzed by normalizing the peak amplitude of all evoked movements to the average baseline. Baseline values were calculated as the average of two baseline sessions (Baseline 1 and Baseline 2), with all subsequent forelimb movement peak amplitudes—including baseline points—divided by this average. This normalization ensured a consistent reference, with baseline points resulting in a normalized value of 1.

During each probing session, a 5 ms optogenetic stimulation burst was delivered every second for a total of 10 stimulations, and the peak amplitude (maximum pixel displacement) of each evoked movement was recorded. Probing sessions were conducted at baseline and at multiple time points post-stimulation (0–40 minutes or 0–85 minutes, depending on the experiment). Mice were randomized weekly to receive either iTBS, cTBS, or Sham stimulation, with a one-week gap between sessions to eliminate potential carryover effects of anesthesia or optogenetic stimulation. Each mouse contributed data to two stimulation conditions, with group assignments determined using a custom R-based randomization script.

2.10.2 EEG Analysis

To adjust the EEG recordings, we first calculated a baseline voltage by taking the median of the EEG signal during a defined pre-stimulation period (from 0.1 seconds before the stimulation to the moment stimulation begins). This baseline represents the typical EEG voltage change before stimulation. Each subsequent voltage point in the recording was then adjusted relative to this baseline to normalize the data for analysis.

Metrics derived from the pre-stimulation EEG recordings were normalized relative to their averaged pre-stimulation value. This was done by calculating the average of the pre-stimulation metrics and then determining the percentage difference between post-stimulation metrics and this baseline average. This normalization ensures a consistent comparison of EEG metrics before and after stimulation.

Depolarization in the EEG is indicated by a reduction in voltage. The maximum depolarization point was identified as the lowest voltage recorded after the onset of stimulation. The time at which this minimum voltage occurred was defined as the depolarization latency.

Polarization latency was defined as the latest time point during the recording at which the EEG voltage was below zero. This measurement reflects the duration of time the signal remained below the baseline threshold.

Hyperpolarization, which occurs as the voltage increases after depolarization, was measured by identifying the maximum voltage recorded after the depolarization phase. The time at which this maximum occurred provides information on the recovery dynamics following depolarization.

2.10.3 Blood Flow Analysis

Blood flow data were collected using LDI software and processed using Python. Full-size plots were generated to visualize blood flow over time, with stimulation points clearly marked by dotted red lines to indicate the onset of stimulation. To quantify blood flow changes, the average blood flow during each stimulation cycle was calculated and normalized to the average flow during a 10-second baseline period immediately preceding the stimulation cycle. Normalized

values for each cycle were grouped by treatment condition (iTBS, cTBS, or Sham) for subsequent analysis.

2.10.4 LBMM Analysis

LBMM data were processed and analyzed using custom MATLAB scripts to generate heat maps of cortical motor representations, with forelimb movement amplitudes measured at each stimulation site. Quantitative metrics such as map size, maximum pixel intensity, and total number of active pixels were derived from these maps. Statistical bar plots were generated using Prism 10.

2.10.5 Statistical Testing

Two-way repeated measures ANOVA was used to assess the main effects of time, treatment group (iTBS, cTBS, or Sham), and their interaction on evoked forelimb movement amplitudes and normalized cortical blood flow. Where appropriate, Greenhouse-Geisser correction was applied when the sphericity assumption was violated. For comparisons involving more than two groups without repeated measures, one-way ANOVA was used. Post-hoc analyses were performed using Šidák's or Tukey's multiple comparisons tests, depending on the context, to determine specific differences between conditions. For non-parametric within-group comparisons against baseline, Wilcoxon signed-rank tests were used. Statistical significance was defined as $p < 0.05$.

3.0 Results

3.1 Ketamine administered via an automated infusion pump ensures stable anesthesia and consistent optogenetically evoked forelimb movement

To ensure consistent and stable anesthesia levels during optogenetic experiments, we systematically evaluated the effects of different ketamine dosing protocols on optogenetically evoked forelimb movements, a measure of MCX activation. Here, "top-ups" refer to supplemental doses of ketamine administered during the experimental procedure to maintain a consistent plane of anesthesia. The goal of this evaluation was to identify a dosing protocol that minimizes variability in motor responses and optimizes conditions for reliable optogenetic stimulation.

To test the stability of anesthesia, we stimulated a single point in the center of the right M1 in all mice using a range of laser powers (0.5–8.7 mW) and quantified the size of the evoked forelimb movements over time (maximum amplitude reached). Three dosing protocols were tested: (1) no supplemental ketamine doses ("no top-ups"), (2) manual ketamine injections at regular intervals based on tail or toe pinch responses ("manual top-ups"), and (3) continuous ketamine infusion via a custom-built automated pump set to a rate of 3 μL/min ("automated infusion").

Effect of No Supplemental Dosing (Group 1)

In mice that did not receive supplemental ketamine doses after the initial injection (Group 1, Fig. 2A; n = 3), forelimb movements evoked by optogenetic stimulation of the motor cortex increased significantly after 30 minutes (Fig. 2D). This increase suggests that the animals became progressively more lightly anesthetized as the initial dose of ketamine was metabolized. This

pattern highlights the challenge of maintaining a stable depth of anesthesia without additional dosing during experiments that extend beyond 30 minutes.

Effect of Manual Supplemental Dosing (Group 2)

In the second group of mice, where ketamine was manually administered at approximately 10-minute intervals based on the response to a tail or toe pinch (Group 2, Fig. 2B; n = 5), forelimb movements evoked by motor cortical stimulation remained stable throughout the 45-minute observation period (Fig. 2E). Statistical analysis using two-way repeated measures ANOVA revealed a significant main effect of laser power on forelimb movement amplitudes ($(F(4, 20) = 9.7, p < 0.001$), confirming that higher light powers elicited stronger movements. In contrast, no significant interaction between time and group was observed ($F(20, 100) = 0.306, p = 0.998$), and the main effect of time alone was also not significant ($F(1.772, 35.44) = 1.242, p = 0.297$, with Greenhouse-Geisser correction $\varepsilon = 0.3544$), indicating that movement amplitudes were stable across the 45-minute duration. Post-hoc comparisons at the 45-minute time point identified significant differences between 0.65 mW and higher powers (4.3 mW, 6.42 mW, and 8.58 mW; $p = 0.030$, 0.033, and 0.027, respectively), with corresponding confidence intervals not overlapping zero. These results demonstrate that manual dosing effectively maintains a consistent plane of anesthesia but requires close monitoring to ensure accurate timing and dosing.

Effect of Automated Ketamine Infusion (Group 3)

In the third group, ketamine was continuously delivered via an automated infusion pump at a fixed rate of 3 μL/min (Group 3, Fig. 2C; n = 8). This method resulted in stable forelimb movements across all time points (Group 2) (Fig. 2F). Repeated measures ANOVA confirmed a

significant main effect of laser power on forelimb movements ($F(4, 35) = 16.83$, $p < 0.001$), consistent with findings in Group 2, indicating that higher light powers reliably produced stronger evoked forelimb response. No significant interaction was found between time and group ($F(36, 315) = 0.399$, $p > 0.999$), nor was the main effect of time alone statistically significant ($F(3.086, 108.0) = 2.118$, $p = 0.078$, with Greenhouse-Geisser correction $\varepsilon = 0.3429$), supporting the observation that evoked movement amplitudes remained stable over the course of the session. Post-hoc Bonferroni comparisons revealed several significant differences between lower and higher laser powers (e.g., 0.5 mW vs. 6.5 mW and 8.7 mW at 30, 40, 45, and 75 minutes; p values ranging from 0.035 to <0.001), reinforcing the effect of laser power. These findings indicate that continuous infusion ensures a consistent depth of anesthesia while supporting reliable stimulation-evoked responses.

Together, these results demonstrate that an automated infusion pump, like manual ketamine dosing, can effectively stabilize anesthesia during optogenetic experiments while eliminating the need for experimenter intervention.

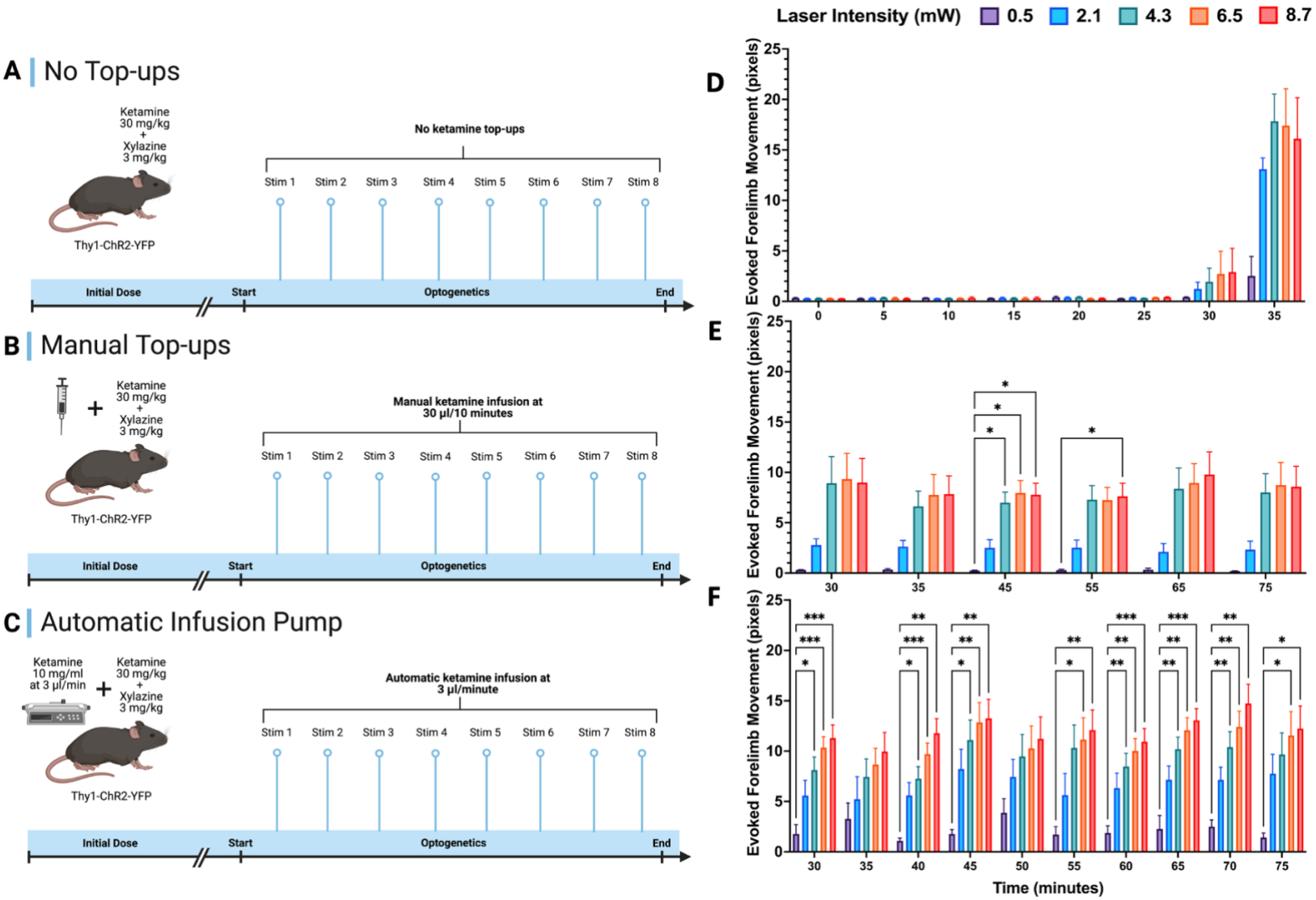

Figure 2. Ketamine management strategies. A. Represents mice (group 1) receiving an initial dose of K/X without any subsequent top-ups. **B.** Depicts mice (group 2) receiving an initial dose of K/X followed by manual IP-injected Ketamine top-ups. **C.** Illustrates mice (group 3) receiving an initial dose of K/X accompanied by automated IP-injected Ketamine top-ups. **D.** Impact of Single Dose K/X Without Top-ups on Evoked Forelimb Movement. This graph demonstrates the effect of a single dose of K/X on evoked forelimb movement in mice recorded up to 35 minutes at five different laser powers post-initial dose. **E.** Effect of Manual Ketamine Top-ups on Evoked Forelimb Movement. Shows the impact of manually injected Ketamine top-ups on evoked forelimb movement in mice, recorded up to 45 minutes at different laser powers following the initial dose of K/X and Ketamine top-ups. **F.** Automated Ketamine Top-ups and Evoked Forelimb Movement. Displays the effect of automated Ketamine top-ups on evoked forelimb movement in mice, measured up to 45 minutes at various laser powers after the initial K/X dose and automatic IP Ketamine top-ups. Created with BioRender.com

3.2 iTBS produces a lasting increase in the amplitude of the optogenetically evoked forelimb movements

To evaluate the effects of iTBS on M1 plasticity, we employed a cohort of nine mice, each undergoing two rounds of randomized treatment (iTBS n = 6, and Sham n = 6). iTBS was delivered to a predefined point in M1 at an intensity of 80% of the resting motor threshold (RMT), determined by the minimum laser power required to elicit consistent forelimb movement (Fig. 3A). To assess changes in motor output, we quantified the magnitude of optogenetically evoked forelimb movements (maximum amplitude reached) before and after iTBS using a consistent suprathreshold laser intensity (~6.5 mW). This is referred to as a probing session. Additionally, we used LDI to measure iTBS-induced changes in blood flow at the stimulation site by continuously recording blood flow before, during, and after iTBS.

Increased Amplitude in the Optogenetically Evoked Motor Output Following iTBS

Mice receiving iTBS exhibited a significant enhancement in normalized evoked forelimb movement compared to sham-treated mice (Fig. 3B). Movement was maintained over the 40-minute post-stimulation observation period. Statistical analysis using two-way repeated measures ANOVA revealed a significant interaction between time and treatment group ($F(8, 80) = 4.0$, $p < 0.001$), as well as significant main effects of time ($F(2.813, 28.13) = 3.32$, $p = 0.022$, with Greenhouse-Geisser correction $\varepsilon = 0.3517$) and treatment group ($F(1, 10) = 11.6$, $p = 0.007$), indicating that the effects of iTBS evolved over time and differed significantly from sham. Post-hoc Fisher's LSD comparisons showed that iTBS-treated mice exhibited significantly greater movement than sham-treated controls at several post-stimulation time points, specifically from minutes 5 ($p = 0.043$) and 10 ($p = 0.037$) through 40 minutes ($p = 0.047$), with the most robust effects observed between 20 and 35 minutes ($p < 0.015$ to 0.004). The mean difference in evoked

movement between the iTBS and sham groups was −2.268 (95% CI: −3.747 to −0.7899), confirming a reliable group-level difference. These findings suggest that iTBS induces a lasting facilitation of motor output, consistent with its known long-term potentiation (LTP)-like effects.

Optogenetically Evoked EEG Response Remain Unaltered Following iTBS

To further investigate the physiological impact of iTBS, we recorded EEG signals from the stimulated hemisphere (right M1) before and after stimulation (Fig. 3C). Single-pulse optogenetic stimulation evoked a characteristic deflection in the EEG trace, which we analyzed using three key metrics: upward peak amplitude, downward peak amplitude, and peak-to-peak amplitude relative to baseline. No significant changes in these metrics were observed following iTBS, indicating that the observed motor enhancements were not accompanied by detectable alterations in cortical EEG responses.

LDI Responses to iTBS

LDI recordings demonstrated that iTBS significantly increased cortical blood flow at the stimulation site compared to sham stimulation. This increase was observed during the 20 cycles of stimulation, with blood flow measurements showing sustained elevations throughout iTBS (Fig. 4B). A Wilcoxon Signed Rank Test confirmed that the increase in blood flow was statistically significant for both sham ($W = 66.0$, $p = 0.0010$) and iTBS ($W = 120.0$, $p < 0.0001$) groups when compared to a theoretical median of zero, indicating that both conditions induced measurable deviations from baseline. However, the actual median change in blood flow for the iTBS group (1.162) was greater than that of the sham group (0.9992), confirming a stronger effect in the iTBS condition. These findings indicate that iTBS induces an upward increase in blood flow compared to Sham.

These results demonstrate that iTBS applied to the MCX enhances optogenetically evoked motor output, as evidenced by increased forelimb movement magnitude. However, this enhancement occurs without measurable changes in EEG deflection metrics, suggesting that iTBS may selectively modulate motor circuit plasticity at levels that may not be detectable by gross cortical EEG recordings.

3.3 The second round of iTBS demonstrates no additional effects on evoked forelimb movement or blood flow

The primary goal of this experiment was to determine whether adding a second round of iTBS, which we would refer to as the Stim 2 period, delivered 40 minutes after the first, could potentiate blood flow responses induced by the initial iTBS session. To test this hypothesis, mice were randomly assigned to one of three groups: iTBS, cTBS, or Sham. As in the previous experiment, all mice underwent baseline optogenetic probing to measure evoked forelimb movements and EEG responses. Following this baseline period, the assigned stimulation protocol (iTBS, cTBS, or Sham) was delivered, and the LDI responses were recorded as depicted in Fig. 4D. This period is called the “Stim 1” session.

Forty minutes after the initial stimulation, all groups received a second round of iTBS, during which the LDI responses were again recorded. This period is called the “Stim 2” period. This was followed by 10 minutes of optogenetic probing to collect evoked forelimb movement and EEG responses. Continuous theta-burst stimulation (cTBS) was included to assess how different TBS protocols influence forelimb movement, cortical EEG signals, and LDI responses. Blood flow responses were measured using LDI during both stimulation sessions and synchronized with optogenetic stimulation to ensure precise temporal alignment with cortical activity.

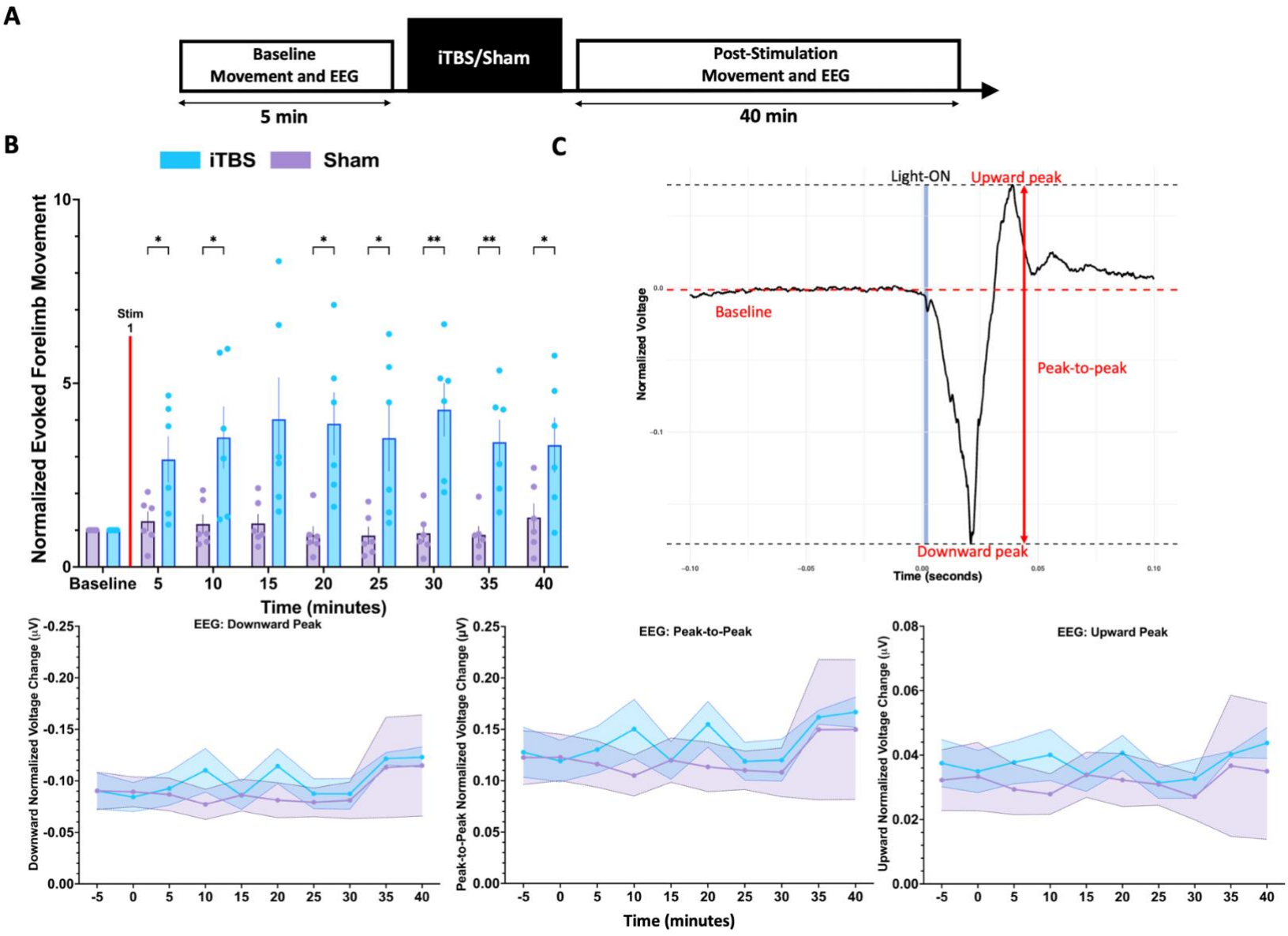

Figure 3. Assessment of Forelimb Movement, EEG, and Cerebral Blood Flow Response to iTBS. A. Experimental Timeline of Treatment and Testing. A timeline showing the sequence of events in the iTBS experiment, including the resting motor threshold determination, baseline recording, iTBS treatment, and subsequent testing intervals. **B.** iTBS produces lasting enhancement of evoked forelimb movements. This shows the normalized contralateral evoked forelimb amplitude in sham and iTBS groups. Each data point represents the average ± SEM of normalized contralateral forelimb movement amplitude (sham n = 6, iTBS n = 6). **C.** EEG recordings show no change in downward, upward, or Peak-to-Peak signals post-iTBS. Each data point represents the average ± SEM of normalized voltage change in downward, upward, and peak-to-peak EEG wave profiles.

LDI Responses to Repeated Stimulation

Analysis of LDI recordings showed that iTBS elicited significantly larger cortical blood flow compared to Sham during the Stim 1 period ($F(5, 46) = 6.9$, $p < 0.0001$; Tukey's post hoc: iTBS vs Sham, $p = 0.0140$, 95% CI [0.02938 to 0.3868]) (Fig. 4E). Forty minutes later, during the Stim 2 period, the blood flow response showed almost no difference when comparing iTBS vs Sham. This indicates that Sham mice receiving iTBS 40 minutes later (during Stim 2 period) exhibited similar blood flow levels to those receiving iTBS during the Stim 1 period. Additionally, there was a reduction in blood flow in the Stim 2 iTBS group compared to iTBS from the Stim 1 group (Mean diff = –0.2315, $p = 0.0093$). No significant differences were observed between Stim 1 Sham vs Stim 2 iTBS or Stim 2 Sham vs Stim 1 iTBS groups.

The attenuation of the blood flow response during the Stim 2 iTBS session corresponds to the lack of further amplitude increase in evoked forelimb movement (Fig. 5B), suggesting a potential relationship between motor output and cerebral blood flow. Meanwhile, mice receiving cTBS during Stim 1 showed an upward increase in blood flow, but during the Stim 2 period, cTBS mice exhibited a decrease in blood flow.

Potentiation of optogenetically evoked Forelimb Movements by Repeated iTBS

The second round of iTBS (Stim 2) showed no change in the amplitude of the optogenetically evoked forelimb movement compared to the first round of iTBS at Stim 1 period (Fig. 5B, Blue bars after the red line vs blue bars after the black line). Nevertheless, mice receiving iTBS showed a significant increase in the optogenetically evoked forelimb movement compared to Sham and cTBS. Statistical analysis using two-way repeated measures ANOVA revealed a significant interaction between time and treatment group ($F(20, 170) = 2.295$, $p = 0.0022$), as

well as main effects of time ($F(1.733, 29.46) = 6.116$, $p = 0.0080$) and group ($F(2, 17) = 15.55$, $p = 0.0001$), with Greenhouse-Geisser correction $\varepsilon = 0.1733$. Post-hoc Tukey comparisons revealed that mice receiving iTBS at Stim 1 period exhibited a significant increase in optogenetically evoked forelimb movement from minutes 5 to 40 ($p < 0.031$, all with 95% CIs not crossing zero), and significantly higher responses than cTBS from minutes 5 through 50 (p values ranging from 0.0140 to 0.0010). Mice in the Stim 2 iTBS group showed a delayed but significant increase from minutes 45 to 50 compared to cTBS ($p = 0.0103$ to 0.0153), despite no significant differences from Sham or the Stim 1 iTBS group at those later time points. In contrast, cTBS did not significantly alter forelimb movement amplitude at any time. These results suggest that iTBS induces robust and sustained motor potentiation, whereas cTBS does not.

Optogenetic Evoked EEG Responses Are Unaffected by Repeated Stimulation

Analysis of EEG signals recorded during the experiment showed no significant changes in evoked cortical responses following Stim 1 iTBS, cTBS, or sham or during Stim 2 (Fig. 5C). Specifically, iTBS did not alter the upward peak, downward peak, or peak-to-peak amplitudes of the EEG signal, even after a second round of iTBS treatment. These findings suggest that iTBS-induced motor potentiation occurs independently of detectable changes in EEG deflection metrics.

3.5 Sustained enhancement of optogenetically evoked motor output following a single round of opto-iTBS persists for 1.5 hours

To evaluate the duration of iTBS effects on motor output, we examined evoked forelimb movements over an extended 85-minute period following a single round of iTBS or sham stimulation. An additional cohort of mice (n = 10) was randomized into two groups, receiving either iTBS (n = 9) or sham treatment (n = 8). Baseline movements were recorded for 5 minutes prior to stimulation to establish pre-stimulation motor activity levels (Fig. 6A). Stimulation was delivered at an intensity calibrated to 80% of the resting motor threshold (RMT), ensuring consistent activation across animals.

Mice receiving iTBS exhibited a significant and sustained increase in normalized evoked forelimb movement compared to the sham group, with the potentiation effect persisting across the entire 85-minute post-stimulation period (Fig. 6B). Statistical analysis using two-way repeated measures ANOVA revealed a significant interaction between time and treatment group ($F(17, 255) = 1.956$, $p = 0.0132$), as well as a main effect of condition ($F(1, 15) = 7.2$, $p = 0.0165$), highlighting the robust and long-lasting impact of iTBS on motor cortex excitability. Post-hoc Šidák comparisons confirmed that the evoked forelimb movements in the iTBS group were significantly greater than those in the sham group at all measured time points, including minutes 5 through 45 ($p < 0.0325$, all with 95% CIs not overlapping zero) and again at minutes 55, 60, 70, and 80 (p-values ranging from 0.0241 to 0.0454). The group difference in overall mean evoked movement amplitude was also significant (mean difference = –3.360, 95% CI [–6.014 to –0.7062], $p = 0.0165$).

These findings demonstrate that a single session of iTBS produces a durable enhancement of motor responses, suggesting that iTBS may induce long-lasting plasticity in motor circuits. In contrast, sham-treated mice displayed stable but significantly lower forelimb movement magnitudes throughout the observation period, indicating the absence of potentiation effects.

Groups	Stim 1	Changes in Blood flow?	Stim 2	Changes in Blood flow?
iTBS	iTBS	Yes	iTBS	No
Sham	Sham	No	iTBS	Yes
cTBS	cTBS	Yes	iTBS	No

Table 1. Summary of LDI recording during Stim 1 and Stim 2 periods. Mice were divided into three groups for Stim 1, during which they were randomized to receive either iTBS, Sham, or cTBS. Forty minutes later, during Stim 2, all mice received iTBS. The table summarizes the changes in cortical blood flow observed during Stim 1 and Stim 2 across the groups.

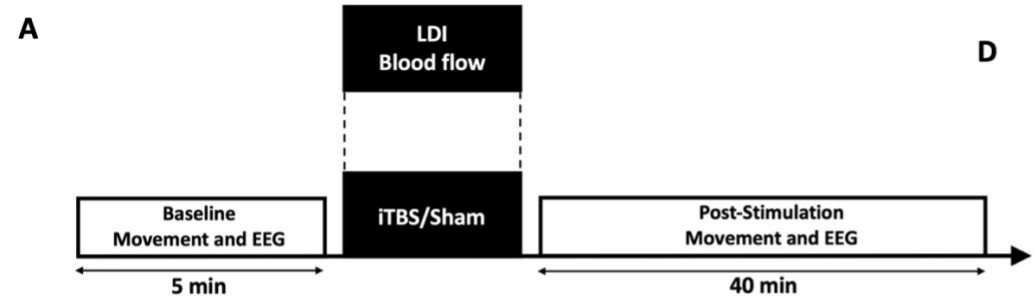
A
LDI
Blood flow
Baseline
Movement and EEG
iTBS/Sham
Post-Stimulation
Movement and EEG
5 min
40 min

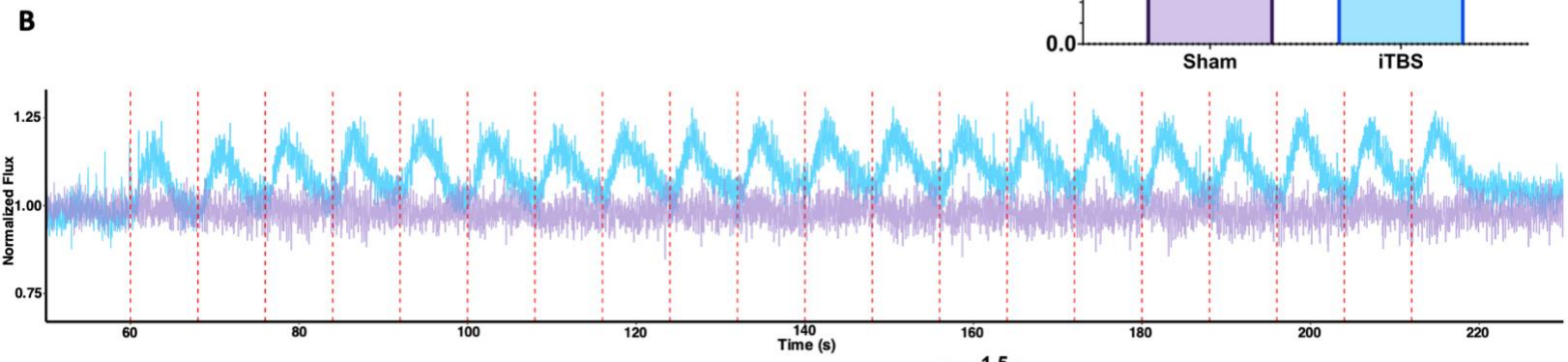
B
Normalized Flux
1.25
1.00
0.75
60
80
100
120
140
160
180
200
220
Time (s)

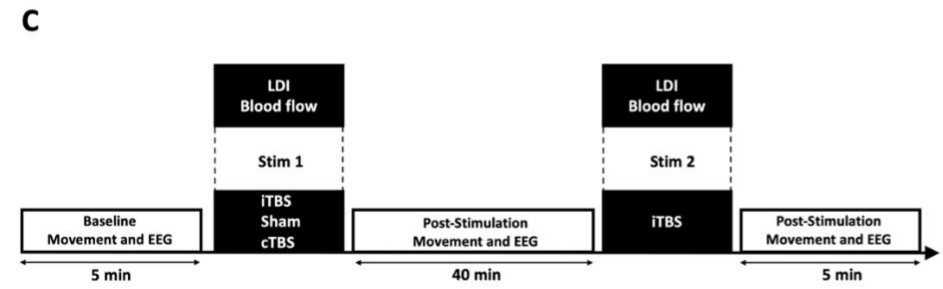
C
LDI
Blood flow
Stim 1
iTBS
Sham
cTBS
LDI
Blood flow
Stim 2
iTBS
Baseline
Movement and EEG
Post-Stimulation
Movement and EEG
Post-Stimulation
Movement and EEG
5 min
40 min
5 min

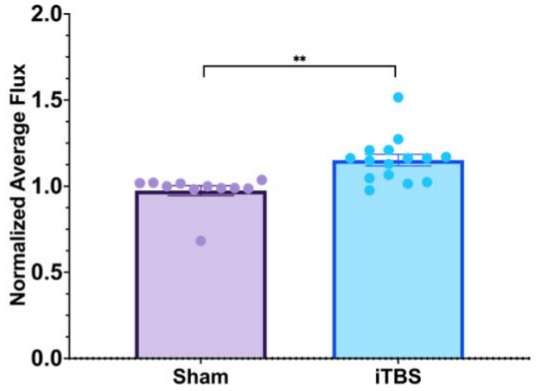
D
Normalized Average Flux
2.0
1.5
1.0
0.5
0.0
**
Sham
iTBS

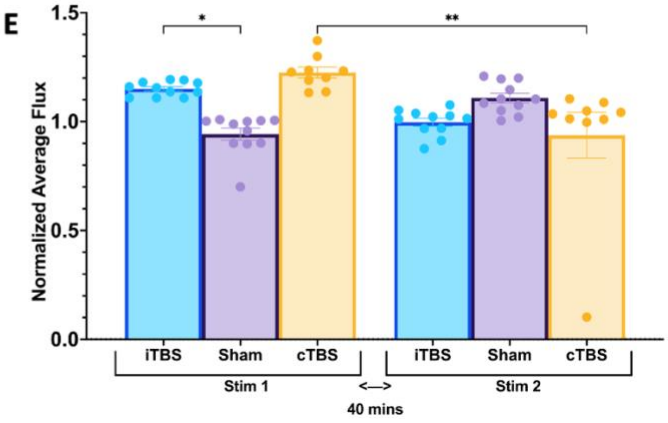
E
Normalized Average Flux
1.5
1.0
0.5
0.0
*
**
iTBS
Sham
cTBS
iTBS
Sham
cTBS
Stim 1
<—>
Stim 2
40 mins

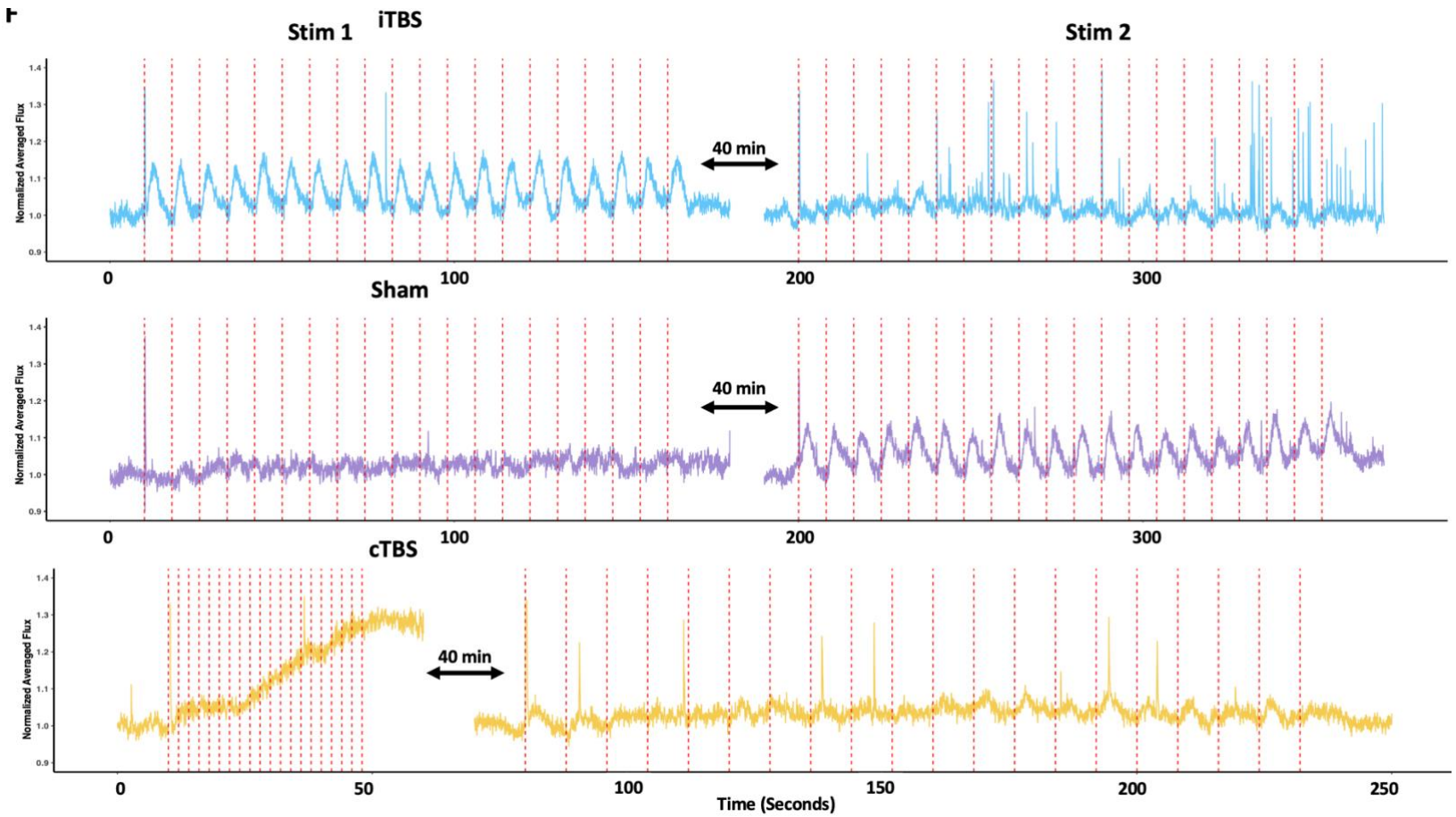

Figure 4. LDF Analysis of Cortical Blood Flow. A. Shows the timeline of the experiment. Mice underwent optogenetic probing to record the evoked forelimb movement and EEG. Then, they were randomized to receive either iTBS or Sham stimulation, followed by a 40-minute optogenetic probing. **B.** Represents averaged normalized blood flow over time during iTBS vs Sham. 10-second baseline recorded before and after. Each red line represents the beginning of the light cycle (total = 20 cycles). **C.** Shows the timeline of the experiment. Mice underwent optogenetic probing to record the evoked forelimb movement and EEG. During Stim 1, mice were randomized to receive iTBS, Sham, or cTBS stimulation, followed by a 40-minute optogenetic probing. After, all mice received iTBS stimulation. This period is referred to as Stim 2. **D.** The bar plot quantifies the normalized averaged blood flow of all cycles in each Sham and iTBS. *$p<0.05$ and **$p<0.002$ denoted significant differences between groups in rmANOVA and post-hoc analysis. **E.** The bar plot shows the quantification of the normalized averaged blood flow for mice that initially received Sham, iTBS, or cTBS, followed by a dose of iTBS 40 minutes later. ***$p<0.001$ denoted significant differences between groups in rmANOVA and post-hoc analysis. **F.** Displays the time course of normalized cortical blood flow recorded during LDI for all groups. Each trace represents the changes in blood flow over time, with vertical red dashed lines indicating the stimulation points.

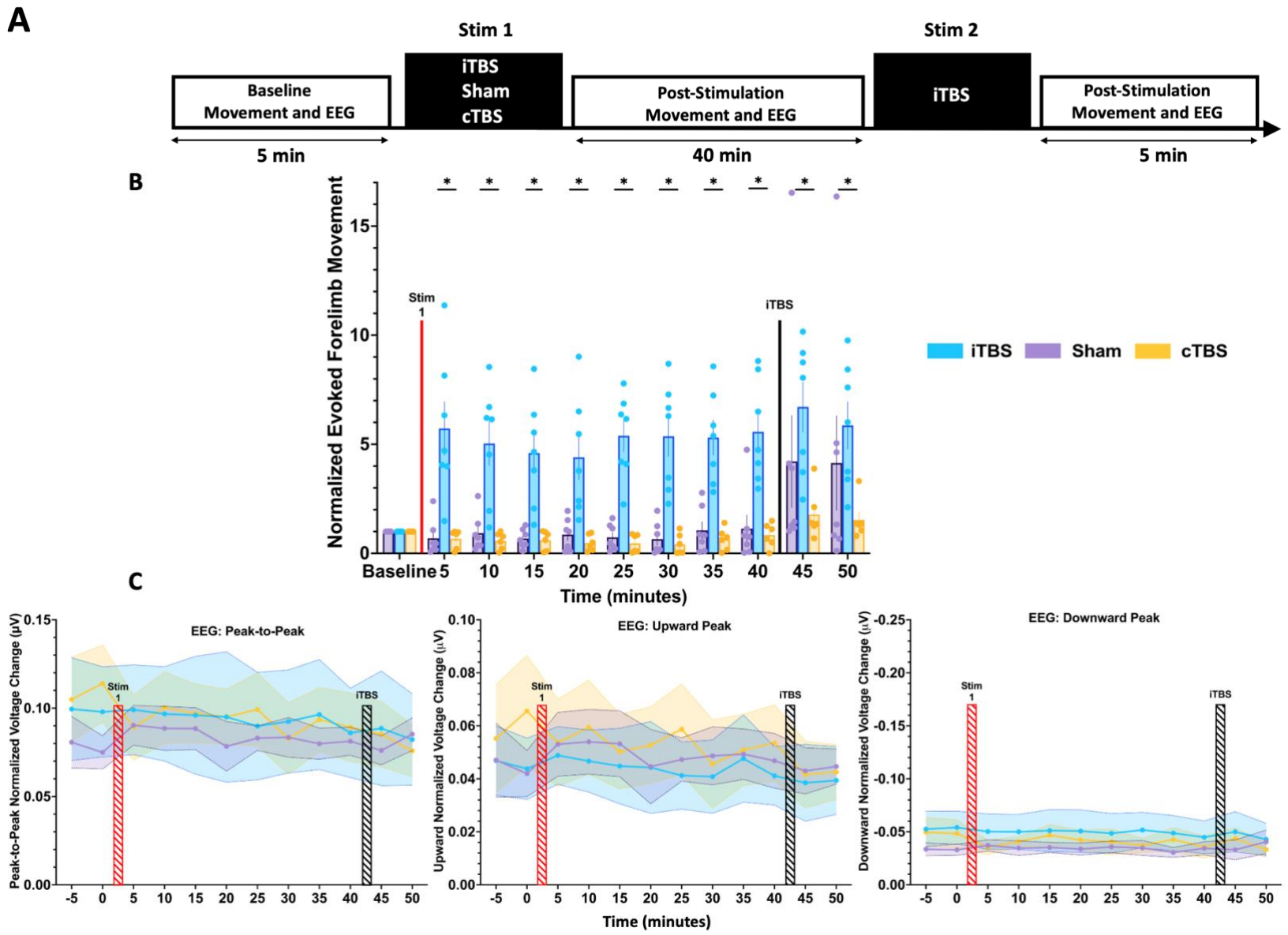

Figure 5. Comparative Dynamics of Forelimb Movement, Blood Flow and EEG Responses to iTBS and cTBS Protocols. A. A timeline showing the sequence of events in the experiment, including the resting motor threshold determination, baseline recording, c/iTBS treatment, and subsequent testing intervals. **B.** Shows the normalized evoked forelimb movement in iTBS (blue), cTBS (yellow), and Sham (purple) groups, indicating significant differences between the groups over time. The red line indicates Stim 1 period which consisted of either (iTBS, Sham, or cTBS). Meanwhile, the black line indicates the Stim 2 period, which only consists of iTBS. * indicates a significant difference among the groups at the specified time point. Detailed significance information: 5 minutes: iTBS vs Sham ($p < 0.05$), iTBS vs cTBS ($p < 0.05$); 10 minutes: iTBS vs Sham ($p < 0.05$), iTBS vs cTBS ($p < 0.01$); 15 minutes: iTBS vs Sham ($p < 0.05$), iTBS vs cTBS ($p < 0.05$); 20 minutes: iTBS vs Sham ($p < 0.05$), iTBS vs. cTBS ($p < 0.05$); 25 minutes: iTBS vs Sham ($p < 0.01$), iTBS vs cTBS ($p < 0.001$); 30 minutes: iTBS vs Sham ($p < 0.01$), iTBS vs cTBS ($p < 0.01$); 35 minutes: iTBS vs Sham ($p < 0.01$), iTBS vs cTBS ($p < 0.01$); 40 minutes: iTBS vs Sham ($p < 0.01$), iTBS vs cTBS ($p < 0.01$); 45 minutes: iTBS vs cTBS ($p < 0.05$); 50 minutes: iTBS vs cTBS ($p < 0.05$).**C.** Shows no change in downward, upward, or Peak-to-Peak signals post any of the treatments.

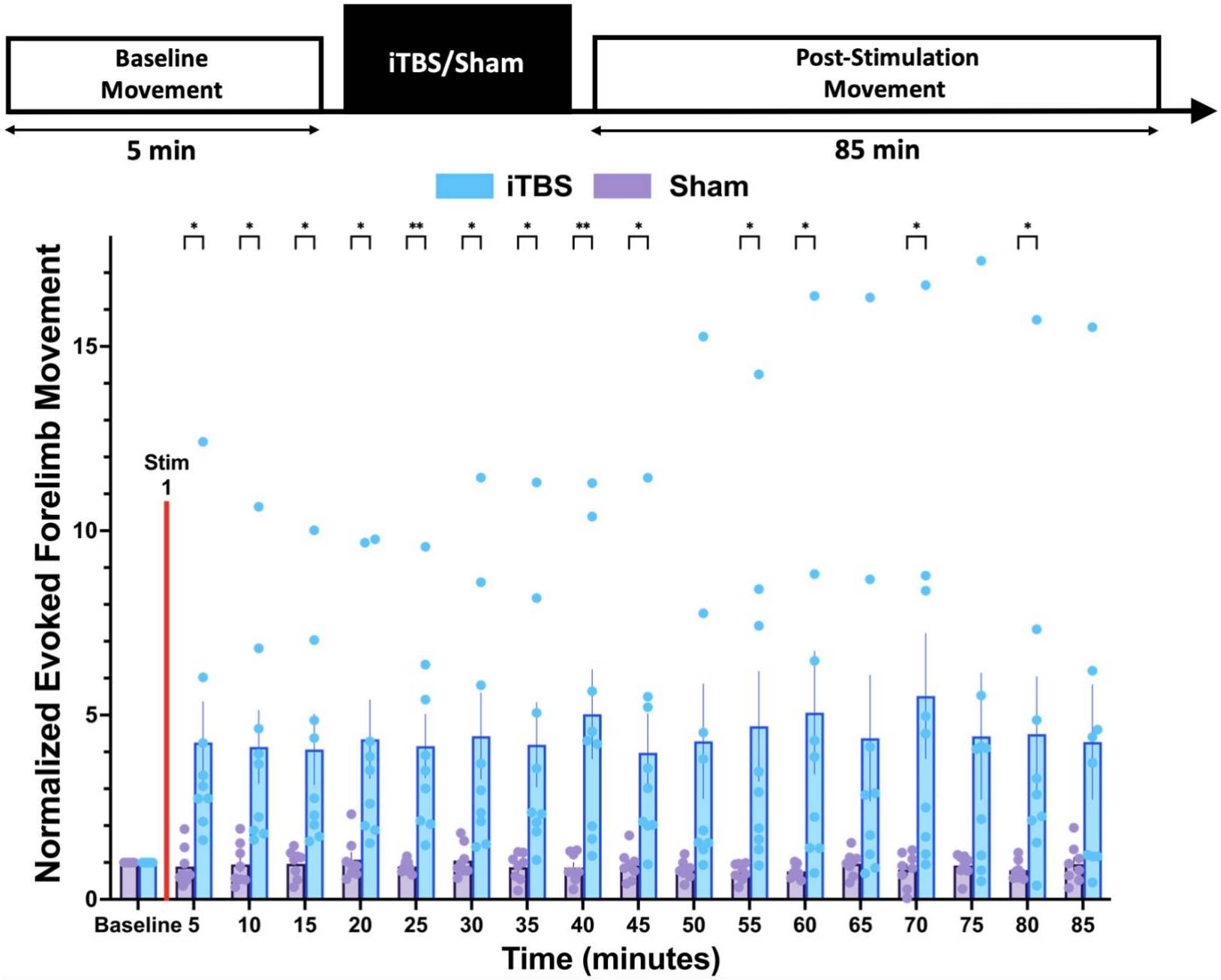

Figure 6. Evoked Forelimb Movement for up to 1.5 hours. iTBS produces lasting enhancement of evoked forelimb movements for 85 minutes post-stimulation. This shows the normalized contralateral evoked forelimb amplitude in sham and iTBS groups. Each data point represents the average ± SEM of normalized contralateral forelimb movement amplitude (sham n = 8, iTBS n = 9).

3.7 iTBS enhances forelimb motor representation in the stimulated (right) hemispheres

To investigate how iTBS modulates the spatial representation of motor output within the cortex, we employed bilateral cortical motor mapping before and after stimulation. This technique allowed us to generate heat maps of evoked forelimb movements across a grid of stimulation points spanning the cortical surface (Fig. 7A). Motor mapping allowed us to examine the spatial extent of potentiation when iTBS was delivered to a single cortical site by comparing pre- and post-stimulation maps, providing insight into how iTBS influences motor representations.

Heat Maps Reveal Expanded Motor Representations Post-iTBS

The motor maps generated from LBMM clearly illustrate the impact of iTBS on motor cortical representations. Warmer colors, representing larger evoked forelimb movement amplitudes, show an expansion in both the amplitude and spatial extent of motor output in the stimulated hemisphere (right) following iTBS (Fig. 7A). This effect was particularly pronounced in regions proximal to the stimulation site but also extended to adjacent cortical areas, suggesting that iTBS enhances not only local cortical excitability but potentially recruits a broader network of motor-related circuits.

Quantitative Analysis Confirms Significant Expansion of Motor Maps

Quantitative analysis of the motor maps provided evidence for the iTBS-induced expansion of motor cortical representations in the stimulated hemisphere. The average number of active pixels, representing the size of the pixel-wise intensity of evoked forelimb movement (Pixel mean), was significantly altered across groups ($F(5, 66) = 3.384$, $p = 0.0088$), with Šidák's post-hoc test showing a significant within-group increase in the iTBS group (mean difference = –

2.433, 95% CI [–4.856 to –0.00877], p = 0.0488) and greater post-stimulation values compared to Sham (mean difference = 2.894, p = 0.0085). The total summed activity (Pixel sum) was significantly different across conditions (F(5, 66) = 2.835, p = 0.0222), with a marked increase in iTBS post-stimulation compared to Sham (mean difference = –539.6, 95% CI [–1019 to –60.02], p = 0.0162)

Similarly, the maximum pixel (Pixel max) intensity, a proxy for the peak amplitude of forelimb movement, was markedly enhanced (F(5, 66) = 2.524, p = 0.0376), indicating increased excitability within the stimulated motor circuits. Post-hoc analysis revealed a statistically significant increase from Sham to iTBS post-stimulation (mean difference = –33.12, 95% CI [–66.21 to –0.027], p = 0.0497).

The overall map size, defined as the total area of the cortical surface contributing to motor output, showed a trend toward significance (F(5, 66) = 2.232, p = 0.0613), with post-hoc analysis revealing a significant difference between the iTBS post-stimulation group and cTBS baseline (mean difference = –8.965, 95% CI [–17.93 to –0.0033], p = 0.0499), suggesting a subtle but statistically detectable expansion of the functional representation area. These quantitative metrics collectively highlight the profound and widespread effects of iTBS on motor cortical plasticity, demonstrating enhanced excitability and reorganization of motor representations within the stimulated hemisphere.

These results demonstrate that a single session of iTBS produces robust and sustained changes in the spatial and functional organization of the motor cortex. The expansion and intensification of motor representations suggest that iTBS enhances both local excitability and the integration of neighboring cortical regions into motor control networks.

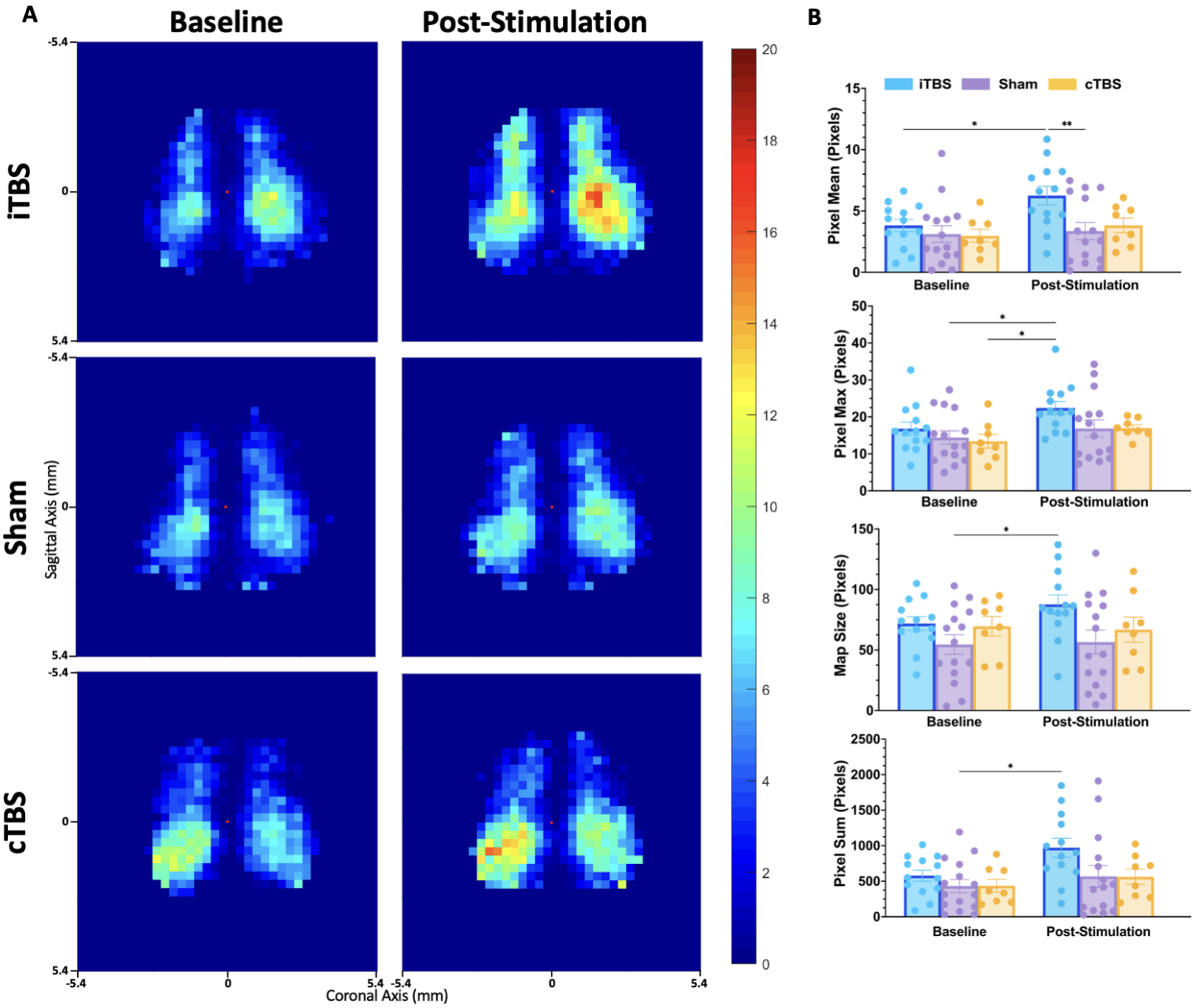

Figure 7. iTBS Effects on Forelimb Motor Representation. This figure depicts the impact of iTBS on the functional organization of the motor cortex, demonstrating changes in forelimb motor representation in the stimulated hemispheres (right). **A.** represents the left forelimb peak movement average at baseline and post-stimulation. **B.** Quantifications of each pixel max, map size, and pixel sum (Pixels). *p<0.05 and **p<0.001 denoted significant differences between groups in one-way ANOVA and post-hoc analysis.

4.0 Discussion

4.1 Overview of thesis findings

This thesis established a noninvasive approach for investigating MCX plasticity using transcranial optogenetics combined with iTBS. Our systematic investigation yielded three principal findings: First, opto-iTBS induced robust and persistent enhancement of motor output, demonstrating successful modulation of targeted motor circuits. Second, the intervention expanded motor representations in the stimulated hemisphere beyond the stimulation period, indicating lasting plasticity effects at the network level. Third, real-time hemodynamic measurements revealed that opto-iTBS elevated cortical blood flow during stimulation, providing direct evidence of successful circuit engagement. The development of standardized anesthesia and noninvasive experimental protocols enabled precise control over stimulation parameters while minimizing confounding variables. Our noninvasive standardized methodological approach and our findings on acute circuit activation and sustained effects establish a foundation for investigating targeted neuromodulation strategies. Our results provide mechanistic insights into activity-dependent MCX plasticity that may inform the development of optimized therapeutic interventions for motor rehabilitation.

4.2 Automated infusion pump

We developed an automated ketamine delivery system to provide consistent anesthesia levels throughout our experiments. To establish this protocol, we first examined how evoked forelimb movements changed over time in response to five different laser powers (0.5-8.7 mW) under three anesthesia conditions. Mice receiving only an initial ketamine dose showed stable responses for 30 minutes, after which movement amplitudes increased significantly, indicating

lighter anesthesia. This observation established the duration of ketamine's initial effect and guided the development of our maintenance protocol.

Based on these findings, we implemented continuous ketamine delivery at three microliters per minute using an automated infusion pump to eliminate potential experimenter bias in anesthesia maintenance. While manual ketamine administration can achieve stable movement responses, the automated system ensures standardization across all experiments, removing any subjective decisions in the timing or volume of supplemental doses. The infusion rate was calibrated to maintain consistent movement amplitudes across all tested laser powers throughout the experimental period. This standardized approach strengthens the reliability of our results by eliminating a potential source of experimental variability in anesthesia depth management.

Before establishing the ketamine protocol, we explored continuous isoflurane administration through a nasal cone. However, this method prevented reliable detection of evoked forelimb movements. The reason is that isoflurane inhibits musculoskeletal responses through its effects on the central nervous system (CNS), peripheral nervous system, and muscle physiology. It enhances inhibitory neurotransmission via $GABA_A$ receptors and suppresses excitatory neurotransmission by inhibiting NMDA receptors, reducing overall motor neuron excitability in the CNS [99,116,117]. At the peripheral level, isoflurane decreases acetylcholine release at the neuromuscular junction, diminishing muscle activation [116,117].

Additionally, it directly stabilizes muscle cell membranes and interferes with calcium release from the sarcoplasmic reticulum, which is crucial for muscle contraction. By suppressing spinal reflex pathways, isoflurane effectively prevents voluntary and reflexive muscle movements,

ensuring comprehensive musculoskeletal suppression during anesthesia. Moreover, based on our experimental observations, isoflurane significantly elevated baseline blood flow levels, making it difficult to detect and quantify evoked hemodynamic responses during laser Doppler imaging. These limitations led us to focus on optimizing injected ketamine anesthesia for our experimental paradigm.

Our implementation of automated ketamine delivery was designed specifically to eliminate potential experimenter bias in anesthesia maintenance. While both manual and automated approaches can maintain stable movement responses, the automated system removes any subjective decision-making in the timing and volume of ketamine administration. This standardization ensures that variations in movement amplitudes can be confidently attributed to our experimental manipulations rather than unconscious experimenter influences on anesthesia management.

4.3 Enhanced motor output and duration

Our experiments demonstrated that opto-iTBS induced sustained enhancement of evoked forelimb movements persisting for 85 minutes post-stimulation. This duration extends beyond the 20–30-minute enhancement window reported in traditional TMS/ICMS/optogenetics protocols. The noninvasive methods in our experimental approach may have contributed to identifying and maintaining these prolonged effects.

The automated ketamine delivery system proved essential in revealing these extended-duration effects. Through initial experiments, we determined that the effects of a single ketamine dose begin to diminish after approximately 30 minutes, resulting in increased forelimb movement

responses. Understanding this timeline was crucial for developing our automated delivery protocol. By initiating automated ketamine infusion immediately after setup, we maintained stable anesthesia levels during this critical 30-minute window and throughout the experiment. The continuous infusion prevents the complete metabolism of ketamine, creating a steady state that maintains consistent movement responses. The reliability of this approach is demonstrated by our sham stimulation group, which showed stable baseline responses throughout the 90-minute recording period. This stability in sham animals confirms that the enhanced movements we observed after iTBS reflect genuine changes in MCX function rather than fluctuations in the anesthesia state.

The noninvasive application of light probing sessions and opto-iTBS allowed us to observe these prolonged effects. Traditional methods requiring invasive procedures trigger inflammatory responses and alter circuit dynamics, interfering with plasticity mechanisms [94,95]. Our transcranial stimulation preserved neural tissue integrity and avoided these confounds. This preservation of circuit dynamics may have contributed to our observation of longer-lasting plasticity effects. The chronic window provided stable optical access without tissue trauma, enabling extended recording sessions without signal degradation.

The cellular specificity achieved through the Thy1-ChR2 mouse line provided precise control over motor circuit activation. The Thy1 promoter drives ChR2 expression specifically in Layer V pyramidal neurons of the MCX [118–120]. These neurons extend their apical dendrites from Layer V up through the superficial layers (I, II, and III) of the cortex [121,122], creating a unique advantage for our transcranial stimulation approach. When blue light penetrates the cranial window and skull, it activates ChR2 channels expressed in these superficial dendrites, generating light-

evoked excitatory responses in Layer V pyramidal neurons without directly affecting surrounding non-ChR2 expressing cells.

This targeted activation of Layer V pyramidal neurons through their apical dendrites provides two key advantages. First, the superficial location of these dendrites enables reliable activation of cortical output neurons through transcranial optogenetic stimulation, circumventing the need for invasive penetration to deeper cortical layers where their cell bodies reside. Second, by restricting ChR2 expression to Layer V pyramidal neurons, we can examine how iTBS specifically modulates these corticospinal and corticocortical pathways. The enhancement of movement responses we observed suggests plasticity in the stimulated cortical circuits. However, future studies will be needed to determine which specific downstream pathways (e.g., corticospinal, corticocortical, or corticothalamic) mediate these behavioral changes.

Response stability throughout the observation period demonstrated consistent potentiation without decay. Our development of high-frame-rate video recording of forelimb movements represents a significant advance over traditional measurement approaches. Unlike EMG recordings, which measure electrical activity from a single muscle through invasive needle electrodes, our method simultaneously captures complete movement trajectories of both forelimbs. EMG electrode placement damages muscle tissue [108,123], compromising the quality of long-term recordings and potentially altering natural movement patterns. In contrast, our video-based approach preserves muscle integrity while comprehensively measuring movement dynamics.

This noninvasive recording method reveals how MCX stimulation affects coordinated forelimb movement. The stability and reliability of these recordings, combined with our precise stimulation targeting and consistent anesthesia, enabled the detection of sustained movement enhancement without the confounding effects of tissue damage. This comprehensive measurement approach strengthens our evidence that iTBS produces lasting changes in motor circuit function, suggesting potential therapeutic applications for enhancing movement recovery.

The sustained enhancement of evoked forelimb movements for 85 minutes reveals new aspects of how the MCX responds to stimulation. Previous studies using invasive methods like ICMS or non-focal TMS reported enhancement lasting only 25-30 minutes [26,52–54,113]. The longer duration we observed likely stems from several advantages of our approach. Traditional invasive methods damage brain tissue during electrode insertion, potentially limiting plasticity mechanisms and masking sustained effects. Even noninvasive approaches like TMS lack spatial precision, activating broad regions of the cortex rather than specific cell populations.

In contrast to iTBS, mice receiving cTBS showed neither enhancement nor reduction in evoked forelimb movements compared to baseline. This observation diverged from previous literature suggesting inhibitory effects of cTBS on motor circuits [15,53]. Notably, in our sequential stimulation experiment (Fig. 4B), mice that received cTBS followed by iTBS at 40 minutes showed no enhancement in evoked forelimb responses to the subsequent iTBS. This resistance to enhancement suggests that while cTBS may not directly inhibit motor output, it might induce mechanisms that prevent subsequent potentiation of motor circuits. The ability of cTBS to block subsequent iTBS-induced enhancement indicates potential metaplastic effects, where initial stimulation alters the threshold for subsequent plasticity induction [81,84].

These findings suggest that we reevaluate current models of how long brain stimulation can maintain enhanced MCX excitability when delivered under controlled conditions.

4.4 Light-Based Motor Maps

LBMM demonstrated increased forelimb movement representations in the MCX after the iTBS application. The motor maps showed increased area and amplitude of evoked movements compared to baseline measurements. Within regions that generated movements at baseline, iTBS significantly enhanced the amplitude of evoked responses across both hemispheres (Fig. 7B). This enhancement suggests strengthening the existing motor circuits within the mapped cortical territory.

The transcranial optogenetic approach enabled precise spatial mapping of motor responses across the cortical surface. By systematically stimulating multiple points within the MCX, we tracked how iTBS altered the spatial organization of movement representations. The observed expansion occurred primarily in regions surrounding the original movement representations, suggesting a gradual recruitment of neighboring cortical territories.

LBMM revealed significant functional changes within the stimulated hemisphere following opto-iTBS. Specifically, we observed both an expansion in the number of responsive cortical sites and increased movement amplitudes at these locations. These findings suggest three key implications for MCX plasticity. First, the expanded motor representations and enhanced responses indicate strengthened functional connectivity within the stimulated region, potentially reflecting increased network excitability. Second, the persistence of these effects for 85 minutes after stimulation

suggests that these functional changes may be supported by structural modifications, though direct confirmation would require additional investigation using techniques such as two-photon imaging to visualize potential synaptic remodeling. Third, the spatial pattern of enhanced responses suggests that iTBS may strengthen intracortical circuits, leading to more robust activation of movement-specific neural networks. This interpretation aligns with our understanding of activity-dependent plasticity in motor circuits, where repeated synchronous activation can enhance synaptic efficacy within functionally connected networks.

In contrast to iTBS, mice receiving cTBS showed no significant changes in motor map size or movement amplitude compared to baseline measurements. This finding parallels our evoked forelimb movement results, where cTBS failed to produce either enhancement or inhibition of movement responses. Previous studies have suggested that cTBS inhibits excitatory networks, reducing movement amplitude. However, our results demonstrate that transcranial optogenetic cTBS neither suppressed nor enhanced motor map parameters. This disparity between our findings and previous literature may stem from differences in stimulation methods or cellular targeting specificity of optogenetic versus electromagnetic approaches.

4.5 LDI Response

Laser Doppler imaging revealed increased cortical blood flow during iTBS delivery to the MCX. Blood flow measurements showed consistent elevation throughout the stimulation period compared to baseline and sham conditions. This increase in blood flow suggests heightened metabolic activity in the stimulated region during iTBS.

Several lines of evidence indicate these blood flow changes reflect genuine neural activity rather than heating effects from light stimulation. While blue light penetrating brain tissue could potentially cause local heating [124–126], the brief light exposure during each iTBS burst could be insufficient to produce significant temperature-related blood flow changes. If heating were responsible for the observed effects, we would expect gradual, sustained increases in blood flow as tissue temperature rose over time. Instead, we observed rapid, dynamic changes in blood flow that corresponded precisely with stimulation timing. These immediate fluctuations in blood flow are characteristic of neurovascular coupling - the brain's natural response to increased neural activity - rather than the slower, progressive changes typically associated with tissue heating.

To investigate whether iTBS could potentiate the hemodynamic response, we compared blood flow changes during a second iTBS stimulation between mice that initially received either iTBS, sham, or cTBS. The blood flow response during the Stim 2 iTBS stimulation showed a visible decrease compared to their initial iTBS response. Furthermore, the Stim 2 iTBS stimulation failed to produce blood flow increases significantly different from sham stimulation, unlike the robust elevation observed during the first iTBS. This attenuation of the hemodynamic response paralleled our findings regarding movement enhancement, where the second iTBS stimulation did not produce additional potentiation of forelimb movements.

The relationship between hemodynamic responses and motor plasticity appears more complex than initially hypothesized. While both iTBS and cTBS induced robust increases in cortical blood flow, their effects on motor output diverged significantly. This dissociation suggests two important mechanistic insights. First, the magnitude of stimulation-induced blood flow changes may not directly determine the direction of plasticity (facilitation versus inhibition). Rather, the

temporal pattern of neuronal activation imposed by different stimulation rhythms likely plays a crucial role in determining the plasticity outcome independent of the concurrent hemodynamic response. The increased blood flow observed during both protocols may simply reflect the heightened metabolic demands of activated neural circuits, while the specific stimulation patterns determine whether the activated circuits undergo long-term potentiation or depression.

Second, this dissociation between blood flow changes and motor outcomes suggests that critical plasticity mechanisms may operate at sites downstream from the stimulated cortical region. While both stimulation protocols induce similar local hemodynamic responses, their divergent effects on motor output could reflect differential modulation of downstream circuits. Several experimental approaches could validate this hypothesis: (1) two-photon imaging of both cortical and subcortical regions to track circuit-specific activation patterns, (2) post-mortem confocal microscopy to examine structural changes throughout the motor network, and (3) quantification of plasticity markers such as BDNF across multiple nodes of the motor circuit. Such analyses could reveal whether differential distribution of plasticity effects, rather than local hemodynamic changes, determines the ultimate impact on motor output.

4.6 EEG

Our EEG recordings during optogenetic stimulation showed consistent electrical responses in the MCX. We analyzed these responses by measuring different components of the EEG wave: the initial downward deflection, upward deflection, and the total peak-to-peak amplitude. Surprisingly, none of these measurements showed significant changes after iTBS compared to baseline recordings, despite clear enhancement of movement responses.

The implementation of EEG recordings was driven by our aim to detect potential changes in electrical activity within the iTBS-stimulated region at high temporal resolution. While EEG signals are inherently complex, we anticipated observable changes based on two key findings: First, LBMM demonstrated enhanced functional connectivity through increased motor representation sites. Second, the elevated neurovascular coupling during iTBS suggested heightened neuronal activity in the stimulated region. However, it is essential to note that these changes in blood flow were primarily observed during high-frequency stimulation protocols (iTBS or cTBS), not during the lower-frequency probing sessions used for movement evocation and EEG response measurement. This temporal distinction in stimulation parameters between the testing and induction phases may account for the differences in observed responses. Further investigation could be done by analyzing EEG signals during iTBS/cTBS.

This lack of change in EEG signals requires careful interpretation due to the nature of epidural recordings. Our electrodes, placed on the brain's surface, collect mixed electrical signals from a broad region of cortical tissue [127–129]. These signals likely combine several types of electrical activity: the initial response of stimulated neurons, the spread of this activity to connected cells, and the return of signals from other brain regions. This mixing of different signal sources, creating a convoluted signal, makes it challenging to identify specific cellular changes that might occur after iTBS.

To better understand these EEG signals, future work should separate them into different frequency components using mathematical analysis, such as a fast Fourier transform. This approach might reveal specific changes hidden within the complex signal. For example, specific

frequencies might represent local circuit activity, while others reflect communication with distant brain regions.

Literature suggests complex patterns of MCX stimulation effects across neural circuits. In human studies, spectral analyses of EEG have revealed frequency-specific effects of iTBS, particularly in modulating specific brain rhythms [130–132]. Additionally, other studies have demonstrated that MCX stimulation can induce changes in subcortical regions, notably the striatum, which receives direct inputs from the MCX [57]. In our study, the persistence of enhanced movements for over an hour suggests plasticity mechanisms operating within either the MCX itself or along the corticospinal pathway. Since Layer V pyramidal neurons in the MCX provide input to the striatum and spinal cord, future investigations should examine how iTBS differentially affects these parallel pathways. This could be approached through spectral analysis of EEG data to detect frequency-band-specific changes, combined recordings from MCX and striatum during and after iTBS, and assessment of plasticity markers along both cortical and subcortical pathways.

5.0 Conclusion

5.1 Preclinical and Clinical Implications

Our findings' implications extend significantly to basic research and clinical applications. Our noninvasive approach overcomes several limitations of traditional methods for studying MCX plasticity. The ability to conduct repeated measurements without tissue damage enables longitudinal studies of plasticity mechanisms. Furthermore, combining multiple complementary measures – movement amplitude, motor mapping, and blood flow – provides a comprehensive understanding of the physiological changes that iTBS induces. These methodological improvements could pave the way for more thorough studies on iTBS, potentially enabling the study of therapeutic protocols that promote stroke rehabilitation for the entire brain function.

These findings suggest relevance for stroke rehabilitation, where the sustained enhancement of motor output and expanded motor representations could facilitate recovery through enhanced circuit recruitment.

5.2 Limitations

Our study has several limitations that should be addressed in future research. While anesthesia was necessary to maintain stable recording conditions, brain activity in anesthetized mice differs from that in awake animals. This difference means that the movement and brain changes we observed might not exactly match what occurs in awake animals performing natural movements.

In this research, we achieved precise control over a specific population of brain cells using light stimulation. However, current clinical brain stimulation methods like TMS affect broader brain

regions [133–135], making it challenging to target specific cell populations with the same precision. This limitation in cellular targeting might influence how effectively our findings translate to clinical applications.

We measured brain changes for up to 85 minutes after stimulation, but questions remain about longer-term effects. Future studies should examine whether repeated stimulation sessions over days or weeks produce lasting improvements in movement ability. Additionally, we focused on measuring basic movement responses rather than complex behaviors. Testing how our stimulation affects skilled movements, such as reaching or grasping, would help determine whether the enhanced responses we observed translate to meaningful improvements in movement control.

5.3 Future Research Directions

Several key research directions emerge from our findings. The sustained enhancement of motor responses lasting over an hour suggests potential structural changes within the MCX. Using two-photon imaging to examine dendritic spine dynamics after iTBS would reveal whether this stimulation induces structural plasticity in MCX circuits. Previous work has shown structural changes in the spinal cord following iTBS, but changes at the cortical level remain unexplored [54,82].

Understanding the full duration of iTBS effects requires the development of new measurement approaches. Current methods rely on anesthesia, limiting our ability to track changes beyond single sessions. Developing reliable techniques for measuring MCX excitability in awake mice would enable investigation of how these effects evolve over days to weeks. This technical

advance would allow optimization of treatment parameters, such as determining ideal intervals between stimulation sessions and the number of sessions needed for maximal benefit.

The most promising direction involves testing iTBS in stroke recovery. The Silasi lab's established photothrombotic stroke model in mice is ideal for examining how iTBS affects injured brain circuits. This work should examine iTBS effectiveness across different stroke recovery phases - acute, subacute, and chronic. Understanding when iTBS produces optimal effects could guide the development of rehabilitation protocols. Additionally, tracking movement recovery following iTBS in stroke mice would reveal whether enhanced MCX responses translate to functional improvements.

These experiments would complete the picture of how iTBS changes brain circuits and influences recovery after injury. The results would guide the development of optimized brain stimulation protocols for stroke rehabilitation.

5.4 Therapeutic Applications

The sustained enhancement of motor responses we observed suggests the potential benefits of combining iTBS with physical rehabilitation. Since our stimulation produced increased movement responses lasting over an hour, this window could allow for targeted motor training when circuits are most responsive to practice. Given that motor training alone induces plasticity, the combination of iTBS-enhanced excitability with specific movement exercises might produce stronger and longer-lasting improvements in motor function.

Questions remain about whether iTBS should be delivered before, during, or after motor training to maximize benefits. The extended duration of motor enhancement we discovered opens new

possibilities for optimizing treatment timing. Additionally, understanding the interaction between daily iTBS sessions and rehabilitation exercises could help establish optimal treatment schedules. For instance, knowing that our stimulation effects last at least 85 minutes provides a defined window for combining iTBS with training exercises. This systematic investigation of treatment timing could lead to more effective rehabilitation protocols for movement recovery.

5.5 Where do we go from here?

This thesis established that opto-iTBS stimulation of the MCX can enhance evoked forelimb movement for up to 85 minutes. This was done by establishing a new, noninvasive metric to quantify these movements by analyzing trajectories using a high frame rate camera in an anesthetized setting. The ability to maintain stable recording conditions through automated anesthesia delivery enabled the detection of these prolonged enhancements in movement responses.

The development of these noninvasive approaches for tracking movement responses, mapping motor regions, and measuring blood flow and EEG activity provides a robust platform for investigating MCX plasticity. This methodological framework opens new avenues for investigating several critical questions: How do different stimulation patterns interact at the circuit level to modulate plasticity? What are the molecular and cellular mechanisms underlying the observed temporal windows of enhanced motor output? How do cortical and subcortical pathways differentially contribute to stimulation-induced plasticity? Addressing these questions will require integrating our cell-specific noninvasive approaches with cellular-resolution imaging, molecular analyses of plasticity markers, and simultaneous recordings from multiple nodes in the motor network. Such investigations will be necessary to understand how the MCX

responds to stimulation like iTBS, optimize stimulation parameters, and develop more effective therapeutic strategies for enhancing motor recovery.

6.0 Supplementary Data:

6.1 Figures

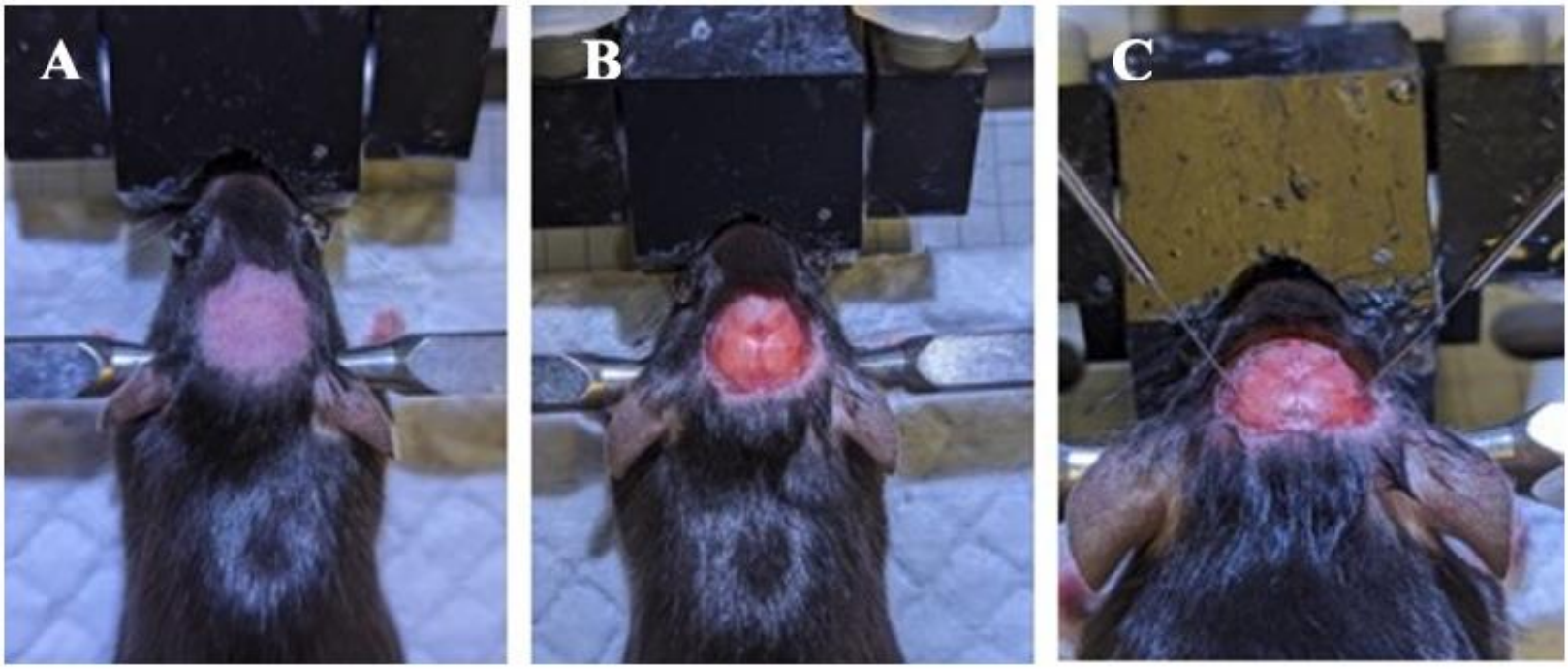

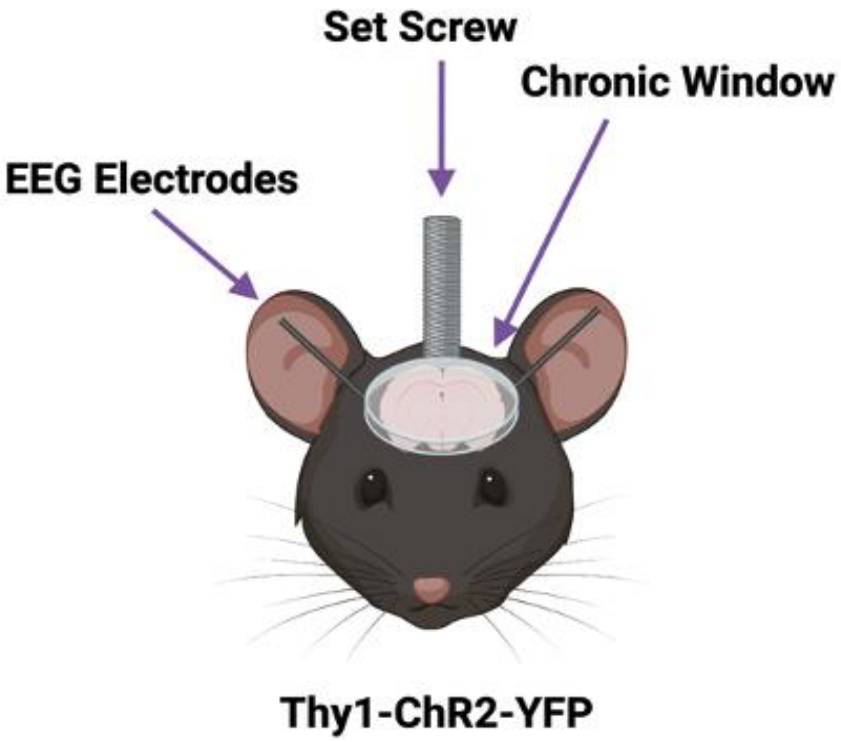

Figure 1. Bilateral cranial window preparation with EEG electrodes. A. Shave the top of the head and remove the skin over both hemispheres. **B.** Apply clear-drying dental cement to the intact skull. **C.** Press a cover glass into the dental cement to make a flat surface. Add EEG electrodes and a head-fixed screw.

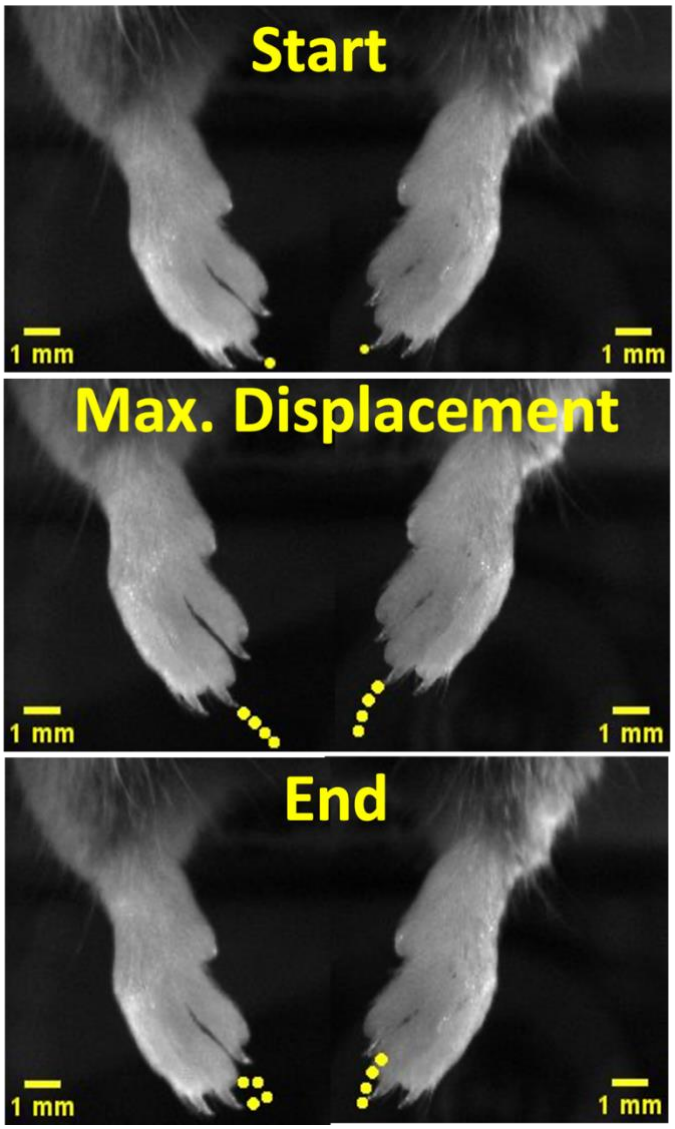

Figure 2. Evoked forelimb movement quantification. This figure demonstrates the evaluation of forelimb movement in response to stimulation, showing the limb's position at rest (Start), its maximum displacement during stimulation (Max. Displacement), and its position at the end of the movement (End), with the extent of movement delineated by dotted lines. When light stimulation is delivered to the MCX, the contralateral forelimb typically exhibits a circular movement pattern, returning to approximately the same starting position after completing a rotation, as illustrated in the bottom image.

7.0 References:

1. Atasavun Uysal, S. & Düger, T. Motor control and sensory-motor integration of human movement. *Comparative Kinesiology of the Human Body: Normal and Pathological Conditions* 443–452 (2020) doi:10.1016/B978-0-12-812162-7.00024-2.
2. Muscles, Nerves and Movement: In Human Occupation - Barbara Tyldesley, June Grieve - Google Books. https://books.google.ca/books?hl=en&lr=&id=64cRjKZnwzUC&oi=fnd&pg=PP5&dq=The+skilled+movements+we+perform+in+our+everyday+lives+are+controlled+by+descending+projections+from+the+brain+that+terminate+at+our+muscles&ots=PsI1LVJ662&sig=7q7IY3JgAQK4oYpjB31jq2oIAhI#v=onepage&q&f=false.
3. Canedo, A. PRIMARY MOTOR CORTEX INFLUENCES ON THE DESCENDING AND ASCENDING SYSTEMS. *Prog Neurobiol* **51**, 287–335 (1997).
4. Waters, R. S., Tamai, Y. & Asanuma, H. Caudal cuneate nucleus projection to the direct thalamic relay to the motor cortex: an electrophysiological study. *Brain Res* **360**, 361–365 (1985).
5. Umeda, T. *et al.* Future spinal reflex is embedded in primary motor cortex output. *Sci Adv* **10**, (2024).
6. Canedo, A. PRIMARY MOTOR CORTEX INFLUENCES ON THE DESCENDING AND ASCENDING SYSTEMS. *Prog Neurobiol* **51**, 287–335 (1997).
7. Pascual-Leone, A. *et al.* Modulation of muscle responses evoked by transcranial magnetic stimulation during the acquisition of new fine motor skills. *https://doi.org/10.1152/jn.1995.74.3.1037* **74**, 1037–1045 (1995).

8. Teka, W. W. *et al.* From the motor cortex to the movement and back again. *PLoS One* **12**, e0179288 (2017).

9. Serradj, N. *et al.* Task-specific modulation of corticospinal neuron activity during motor learning in mice. *Nat Commun* **14**, (2023).

10. Hooks, B. M. Sensorimotor Convergence in Circuitry of the Motor Cortex. *http://dx.doi.org/10.1177/1073858416645088* **23**, 251–263 (2016).

11. Nielsen, J. B. & Cohen, L. G. The olympic brain. Does corticospinal plasticity play a role in acquisition of skills required for high-performance sports? *J Physiol* **586**, 65–70 (2008).

12. Blumberger, D. M. *et al.* Effectiveness of theta burst versus high-frequency repetitive transcranial magnetic stimulation in patients with depression (THREE-D): a randomised non-inferiority trial. *The Lancet* **391**, 1683–1692 (2018).

13. Corp, D. T. *et al.* Large-scale analysis of interindividual variability in theta-burst stimulation data: Results from the 'Big TMS Data Collaboration'. *Brain Stimul* **13**, 1476–1488 (2020).

14. Desmyter, S. *et al.* Accelerated intermittent theta burst stimulation for suicide risk in therapy-resistant depressed patients: A randomized, sham-controlled trial. *Front Hum Neurosci* **10**, 213386 (2016).

15. Huang, Y. Z., Edwards, M. J., Rounis, E., Bhatia, K. P. & Rothwell, J. C. Theta burst stimulation of the human motor cortex. *Neuron* **45**, 201–206 (2005).

16. Huang, Y. Z. & Rothwell, J. C. The effect of short-duration bursts of high-frequency, low-intensity transcranial magnetic stimulation on the human motor cortex. *Clinical Neurophysiology* **115**, 1069–1075 (2004).

17. Canedo, A. PRIMARY MOTOR CORTEX INFLUENCES ON THE DESCENDING AND ASCENDING SYSTEMS. *Prog Neurobiol* **51**, 287–335 (1997).

18. Stinear, C. M. *et al.* Functional potential in chronic stroke patients depends on corticospinal tract integrity. *Brain* **130**, 170–180 (2007).

19. McDonnell, M. N. & Stinear, C. M. TMS measures of motor cortex function after stroke: A meta-analysis. *Brain Stimul* **10**, 721–734 (2017).

20. Noé-Sebastián, E. *et al.* Disability after stroke: A longitudinal study in moderate and severe stroke patients included in a multidisciplinary rehabilitation program. *Rev Neurol* **64**, 385–392 (2017).

21. Grefkes, C., Grefkes, C., Fink, G. R. & Fink, G. R. Recovery from stroke: current concepts and future perspectives. *Neurol Res Pract* **2**, (2020).

22. Grefkes, C., Grefkes, C., Fink, G. R. & Fink, G. R. Recovery from stroke: Current concepts and future perspectives. *Neurol Res Pract* **2**, 1–10 (2020).

23. Siebner, H. R. & Rothwell, J. Transcranial magnetic stimulation: New insights into representational cortical plasticity. *Exp Brain Res* **148**, 1–16 (2003).

24. Bashir, S., Mizrahi, I., Weaver, K., Fregni, F. & Pascual-Leone, A. Assessment and Modulation of Neural Plasticity in Rehabilitation With Transcranial Magnetic Stimulation. *PM&R* **2**, S253–S268 (2010).

25. Cárdenas-Morales, L., Nowak, D. A., Kammer, T., Wolf, R. C. & Schönfeldt-Lecuona, C. Mechanisms and applications of theta-burst rTMS on the human motor cortex. *Brain Topography* vol. 22 294–306 Preprint at https://doi.org/10.1007/s10548-009-0084-7 (2010).

26. Wischnewski, M. & Schutter, D. J. L. G. Efficacy and Time Course of Theta Burst Stimulation in Healthy Humans. *Brain Stimul* **8**, 685–692 (2015).

27. Huang, Y. *et al.* Theta-burst direct electrical stimulation remodels human brain networks. *Nature Communications 2024 15:1* **15**, 1–17 (2024).

28. Rohan, J. G., Carhuatanta, K. A., McInturf, S. M., Miklasevich, M. K. & Jankord, R. Modulating Hippocampal Plasticity with In Vivo Brain Stimulation. *Journal of Neuroscience* **35**, 12824–12832 (2015).

29. Morgan, S. L. & Teyler, T. J. Electrical stimuli patterned after the theta-rhythm induce multiple forms of LTP. *J Neurophysiol* **86**, 1289–1296 (2001).

30. Sweet, J. A., Eakin, K. C., Munyon, C. N. & Miller, J. P. Improved learning and memory with theta-burst stimulation of the fornix in rat model of traumatic brain injury. *Hippocampus* **24**, 1592–1600 (2014).

31. Sheridan, G. K., Moeendarbary, E., Pickering, M., O'Connor, J. J. & Murphy, K. J. Theta-Burst Stimulation of Hippocampal Slices Induces Network-Level Calcium Oscillations and Activates Analogous Gene Transcription to Spatial Learning. *PLoS One* **9**, e100546 (2014).

32. Lowe, C. J., Manocchio, F., Safati, A. B. & Hall, P. A. The effects of theta burst stimulation (TBS) targeting the prefrontal cortex on executive functioning: A systematic review and meta-analysis. *Neuropsychologia* **111**, 344–359 (2018).

33. Chung, S. W. *et al.* Demonstration of short-term plasticity in the dorsolateral prefrontal cortex with theta burst stimulation: A TMS-EEG study. *Clinical Neurophysiology* **128**, 1117–1126 (2017).

34. Kim, J. K. *et al.* Effects of multi-session intermittent theta burst stimulation on central neuropathic pain: A randomized controlled trial. *NeuroRehabilitation* **46**, 127–134 (2020).

35. Voigt, J. D., Leuchter, A. F. & Carpenter, L. L. Theta burst stimulation for the acute treatment of major depressive disorder: A systematic review and meta-analysis. *Translational Psychiatry 2021 11:1* **11**, 1–12 (2021).

36. Wong, J. L. D., Lynch, G. & Larson, J. *Short Communications Patterned Stimulation at the Theta Frequency Is Optimal for the Induction of Hippocampal Long-Term Potentiation*. *Brain Research* vol. 368 (1986).

37. Hess, G. & Donoghue, J. P. Long-term potentiation of horizontal connections provides a mechanism to reorganize cortical motor maps. *https://doi.org/10.1152/jn.1994.71.6.2543* **71**, 2543–2547 (1994).

38. Volz, L. J., Benali, A., Mix, A., Neubacher, U. & Funke, K. Dose-dependence of changes in cortical protein expression induced with repeated transcranial magnetic theta-burst stimulation in the rat. *Brain Stimul* **6**, 598–606 (2013).

39. Hsieh, C. H., Wu, C. W. & Chen, J. J. J. Application of cortical optogenetic stimulation of animal model for modulating motor plasticity. in *IFMBE Proceedings* vol. 52 84–87 (Springer Verlag, 2015).

40. Solomon, E. A. *et al.* Theta-burst stimulation entrains frequency-specific oscillatory responses. *Brain Stimul* **14**, 1271–1284 (2021).

41. Hsieh, T.-H. ; *et al.* Neuromodulatory Responses Elicited by Intermittent versus Continuous Transcranial Focused Ultrasound Stimulation of the Motor Cortex in

Rats. *International Journal of Molecular Sciences 2024, Vol. 25, Page 5687* **25**, 5687 (2024).

42. Vernet, M. *et al.* Insights on the neural basis of motor plasticity induced by theta burst stimulation from TMS–EEG. *European Journal of Neuroscience* **37**, 598–606 (2013).

43. Hsieh, T. H. *et al.* Novel use of theta burst cortical electrical stimulation for modulating motor plasticity in rats. *J Med Biol Eng* **35**, 62–68 (2015).

44. Fu, W. *et al.* Gamma oscillations induced by 40-Hz visual-auditory stimulation for the treatment of acute-phase limb motor rehabilitation after stroke: study protocol for a prospective randomized controlled trial. *Trials* **25**, 1–14 (2024).

45. Muthukumaraswamy, S. D. Functional properties of human primary motor cortex gamma oscillations. *J Neurophysiol* **104**, 2873–2885 (2010).

46. Cheyne, D., Bells, S., Ferrari, P., Gaetz, W. & Bostan, A. C. Self-paced movements induce high-frequency gamma oscillations in primary motor cortex. *Neuroimage* **42**, 332–342 (2008).

47. Ma, R. *et al.* High Gamma and Beta Temporal Interference Stimulation in the Human Motor Cortex Improves Motor Functions. *Front Neurosci* **15**, 800436 (2022).

48. Guerra, A. *et al.* The effect of gamma oscillations in boosting primary motor cortex plasticity is greater in young than older adults. *Clin Neurophysiol* **132**, 1358–1366 (2021).

49. Nudo, R. J., Plautz, E. J. & Milliken, G. W. Adaptive Plasticity in Primate Motor Cortex as a Consequence of Behavioral Experience and Neuronal Injury. *Seminars in Neuroscience* **9**, 13–23 (1997).

50. Blitz, D. M., Foster, K. A. & Regehr, W. G. Short-term synaptic plasticity: a comparison of two synapses. *Nature Reviews Neuroscience 2004 5:8* **5**, 630–640 (2004).

51. Murphy, T. H. & Corbett, D. Plasticity during stroke recovery: from synapse to behaviour. *Nat Rev Neurosci* **10**, 861–872 (2009).

52. Hsieh, T. H. *et al.* Novel use of theta burst cortical electrical stimulation for modulating motor plasticity in rats. *J Med Biol Eng* **35**, 62–68 (2015).

53. Wu, C. W., Chiu, W. T., Hsieh, T. H., Hsieh, C. H. & Chen, J. J. J. Modulation of motor excitability by cortical optogenetic theta burst stimulation. *PLoS One* **13**, (2018).

54. Amer, A. & Martin, J. H. Repeated motor cortex theta-burst stimulation produces persistent strengthening of corticospinal motor output and durable spinal cord structural changes in the rat. *Brain Stimul* **15**, 1013–1022 (2022).

55. Brown, A. R., Mitra, S., Teskey, G. C. & Boychuk, J. A. Complex forelimb movements and cortical topography evoked by intracortical microstimulation in male and female mice. *Cerebral Cortex* **33**, 1866–1875 (2023).

56. Strafella, A. P., Paus, ˇ, Barrett, J. & Dagher, A. Repetitive Transcranial Magnetic Stimulation of the Human Prefrontal Cortex Induces Dopamine Release in the Caudate Nucleus. (2001).

57. Strafella, A. P., Paus, T., Fraraccio, M. & Dagher, A. Striatal dopamine release induced by repetitive transcranial magnetic stimulation of the human motor cortex. *Brain* **126**, 2609–2615 (2003).

58. Ting, W. K. C., Fadul, F. A. R., Fecteau, S. & Ethier, C. Neurostimulation for Stroke Rehabilitation. *Front Neurosci* **15**, 583 (2021).

59. Polanía, R., Nitsche, M. A. & Ruff, C. C. Studying and modifying brain function with non-invasive brain stimulation. *Nature Neuroscience 2017 21:2* **21**, 174–187 (2018).

60. Dayan, E., Censor, N., Buch, E. R., Sandrini, M. & Cohen, L. G. Noninvasive brain stimulation: from physiology to network dynamics and back. *Nature Neuroscience 2013 16:7* **16**, 838–844 (2013).

61. Schulz, R., Gerloff, C. & Hummel, F. C. Non-invasive brain stimulation in neurological diseases. *Neuropharmacology* **64**, 579–587 (2013).

62. Jannati, A., Oberman, L. M., Rotenberg, A. & Pascual-Leone, A. Assessing the mechanisms of brain plasticity by transcranial magnetic stimulation. *Neuropsychopharmacology 2022 48:1* **48**, 191–208 (2022).

63. Wendt, K. *et al.* The effect of pulse shape in theta-burst stimulation: Monophasic vs biphasic TMS. *Brain Stimul* **16**, 1178–1185 (2023).

64. Hallett, M. Transcranial Magnetic Stimulation: A Primer. *Neuron* **55**, 187–199 (2007).

65. Paulus, W. Transcranial brain stimulation: potential and limitations. *e-Neuroforum 2014 5:2* **5**, 29–36 (2014).

66. Latorre, A., Rocchi, L., Berardelli, A., Bhatia, K. P. & Rothwell, J. C. The use of transcranial magnetic stimulation as a treatment for movement disorders: A critical review. *Movement Disorders* **34**, 769–782 (2019).

67. Kim, Y.-H. *et al.* Repetitive Transcranial Magnetic Stimulation-Induced Corticomotor Excitability and Associated Motor Skill Acquisition in Chronic Stroke. (2006) doi:10.1161/01.STR.0000221233.55497.51.

68. Richards, L. G., Stewart, K. C., Woodbury, M. L., Senesac, C. & Cauraugh, J. H. Movement-dependent stroke recovery: A systematic review and meta-analysis of TMS and fMRI evidence. *Neuropsychologia* **46**, 3–11 (2008).

69. Liepert, J. Chapter 37 TMS in stroke. *Suppl Clin Neurophysiol* **56**, 368–380 (2003).

70. Smith, M. C. & Stinear, C. M. Transcranial magnetic stimulation (TMS) in stroke: Ready for clinical practice? *Journal of Clinical Neuroscience* **31**, 10–14 (2016).

71. Smith, M.-C. & Stinear, C. M. Plasticity and motor recovery after stroke: Implications for physiotherapy. *New Zealand Journal of Physiotherapy* **44**, 166–173–166–173 (2016).

72. Marquez, J., van Vliet, P., Mcelduff, P., Lagopoulos, J. & Parsons, M. Transcranial direct current stimulation (tDCS): Does it have merit in stroke rehabilitation? A systematic review. *International Journal of Stroke* **10**, 306–316 (2015).

73. Orrù, G., Conversano, C., Hitchcott, P. K. & Gemignani, A. Motor stroke recovery after tDCS: A systematic review. *Rev Neurosci* **31**, 201–218 (2020).

74. Nitsche, M. A. & Paulus, W. Transcranial direct current stimulation – update 2011. *Restor Neurol Neurosci* **29**, 463–492 (2011).

75. Ozen, S. *et al.* Transcranial Electric Stimulation Entrains Cortical Neuronal Populations in Rats. *Journal of Neuroscience* **30**, 11476–11485 (2010).

76. Vöröslakos, M. *et al.* Direct effects of transcranial electric stimulation on brain circuits in rats and humans. *Nature Communications 2018 9:1* **9**, 1–17 (2018).

77. Tang, Z. *et al.* An Optic Nerve Crush Injury Murine Model to Study Retinal Ganglion Cell Survival. *JoVE (Journal of Visualized Experiments)* e2685 (2011) doi:10.3791/2685.

78. Hensel, L. *et al.* Intermittent theta burst stimulation applied during early rehabilitation after stroke: Study protocol for a randomised controlled trial. *BMJ Open* **9**, (2019).

79. Chen, Y. J. *et al.* Intermittent theta burst stimulation enhances upper limb motor function in patients with chronic stroke: A pilot randomized controlled trial. *BMC Neurol* **19**, 1–10 (2019).

80. Hsu, Y. F. *et al.* Intermittent theta burst stimulation over ipsilesional primary motor cortex of subacute ischemic stroke patients: A pilot study. *Brain Stimul* **6**, 166–174 (2013).

81. Larson, J. & Munkácsy, E. Theta-burst LTP. *Brain Research* vol. 1621 38–50 Preprint at https://doi.org/10.1016/j.brainres.2014.10.034 (2015).

82. Amer, A., Xia, J., Smith, M. & Martin, J. H. Spinal cord representation of motor cortex plasticity reflects corticospinal tract LTP. **118**, (2021).

83. Goldsworthy, M. R., Müller-Dahlhaus, F., Ridding, M. C. & Ziemann, U. Resistant Against De-depression: LTD-Like Plasticity in the Human Motor Cortex Induced by Spaced cTBS. *Cerebral Cortex* **25**, 1724–1734 (2015).

84. Suppa, A. *et al.* Primary motor cortex LTP/LTD-like plasticity in probable corticobasal syndrome. *J Neurophysiol* **115**, 717–727 (2016).

85. Floel, A. & Cohen, L. G. Recovery of function in humans: Cortical stimulation and pharmacological treatments after stroke. *Neurobiol Dis* **37**, 243–251 (2010).

86. Ngetich, R., Zhou, J., Zhang, J., Jin, Z. & Li, L. Assessing the Effects of Continuous Theta Burst Stimulation Over the Dorsolateral Prefrontal Cortex on Human Cognition: A Systematic Review. *Front Integr Neurosci* **14**, 529823 (2020).

87. Grefkes, C. & Fink, G. R. Connectivity-based approaches in stroke and recovery of function. *Lancet Neurol* **13**, 206–216 (2014).

88. Bakulin, I. *et al.* Adding a Second iTBS Block in 15 or 60 Min Time Interval Does Not Increase iTBS Effects on Motor Cortex Excitability and the Responder Rates. *Brain Sci* **12**, (2022).

89. Martin, C. Contributions and complexities from the use of in-vivo animal models to improve understanding of human neuroimaging signals. *Front Neurosci* **8**, 91140 (2014).

90. Song, W., Amer, A., Ryan, D. & Martin, J. H. Combined motor cortex and spinal cord neuromodulation promotes corticospinal system functional and structural plasticity and motor function after injury. *Exp Neurol* **277**, 46–57 (2016).

91. Nudo, R. J., Jenkins, W. M. & Merzenieh, M. M. Repetitive Microstimulation Alters the Cortical Representation of Movements in Adult Rats. *Somatosens Mot Res* **7**, 463–483 (1990).

92. Frost, S. B. *et al.* Reorganization of Ventral Premotor Cortex After Ischemic Brain Injury: Effects of Forced Use. *Neurorehabil Neural Repair* **36**, 514–524 (2022).

93. Urban, E. T. *et al.* Corticocortical connections of the rostral forelimb area in rats: a quantitative tract-tracing study. *Cerebral Cortex* **34**, (2024).

94. Rajan, A. T. *et al.* The effects of chronic intracortical microstimulation on neural tissue and fine motor behavior. *J Neural Eng* **12**, 066018 (2015).

95. Carè, M. *et al.* The impact of closed-loop intracortical stimulation on neural activity in brain-injured, anesthetized animals. *Bioelectron Med* **8**, 1–14 (2022).

96. Hoffmann, U., Sheng, H., Ayata, C. & Warner, D. S. Anesthesia in Experimental Stroke Research. *Translational Stroke Research 2016 7:5* **7**, 358–367 (2016).

97. Traystman, R. J. Effect of Anesthesia in Stroke Models. *Neuromethods* **47**, 121–138 (2010).

98. Hohlbaum, K. *et al.* Impact of repeated anesthesia with ketamine and xylazine on the well-being of C57BL/6JRj mice. *PLoS One* **13**, e0203559 (2018).

99. David, E. M., Pacharinsak, C., Jampachaisri, K., Hagan, L. & Marx, J. O. Use of Ketamine or Xylazine to Provide Balanced Anesthesia with Isoflurane in C57BL/6J Mice. *Journal of the American Association for Laboratory Animal Science* **61**, 457–467 (2022).

100. Williams, S. C. P. & Deisseroth, K. Optogenetics. *Proc Natl Acad Sci U S A* **110**, 16287 (2013).

101. Deisseroth, K. Optogenetics. *Nature Methods 2011 8:1* **8**, 26–29 (2010).

102. Duebel, J., Marazova, K. & Sahel, J. A. Optogenetics. *Curr Opin Ophthalmol* **26**, 226 (2015).

103. Yizhar, O., Fenno, L. E., Davidson, T. J., Mogri, M. & Deisseroth, K. Optogenetics in Neural Systems. *Neuron* vol. 71 9–34 Preprint at https://doi.org/10.1016/j.neuron.2011.06.004 (2011).

104. Zeng, H. & Madisen, L. Mouse transgenic approaches in optogenetics. *Prog Brain Res* **196**, 193 (2012).

105. Herreras, O. Local field potentials: Myths and misunderstandings. *Front Neural Circuits* **10**, 205896 (2016).

106. Haumesser, J. K. *et al*. Acute In Vivo Electrophysiological Recordings of Local Field Potentials and Multi-unit Activity from the Hyperdirect Pathway in Anesthetized Rats. *J Vis Exp* **2017**, 55940 (2017).

107. Hyland, B. I. & Jordan, V. M. B. Muscle activity during forelimb reaching movements in rats. *Behavioural Brain Research* **85**, 175–186 (1997).

108. Cohen, A. H. & Gans, C. Muscle activity in rat locomotion: Movement analysis and electromyography of the flexors and extensors of the elbow. *J Morphol* **146**, 177–196 (1975).

109. Bijsterbosch, J. D., Barker, A. T., Lee, K. H. & Woodruff, P. W. R. Where does transcranial magnetic stimulation (TMS) stimulate? Modelling of induced field maps for some common cortical and cerebellar targets. *Med Biol Eng Comput* **50**, 671–681 (2012).

110. Hussin, A. T., Boychuk, J. A., Brown, A. R., Pittman, Q. J. & Campbell Teskey, G. Intracortical Microstimulation (ICMS) Activates Motor Cortex Layer 5 Pyramidal Neurons Mainly Transsynaptically. *Brain Stimul* **8**, 742–750 (2015).

111. LaPallo, B. K., Wolpaw, J. R., Chen, X. Y. & Carp, J. S. Long-term recording of external urethral sphincter EMG activity in unanesthetized, unrestrained rats. *Am J Physiol Renal Physiol* **307**, 485–497 (2014).

112. Kristl, A. C., Akay, T. & Miri, A. Recording Forelimb Muscle Activity in Head-Fixed Mice with Chronically Implanted EMG Electrodes Recording Forelimb Muscle Activity in Head-Fixed Mice with Chronically Implanted EMG Electrodes Corresponding Author Date Published. *Article in Journal of Visualized Experiments* 66584 (2024) doi:10.3791/66584.

113. Di Lazzaro, V. *et al.* The physiological basis of the effects of intermittent theta burst stimulation of the human motor cortex. *Journal of Physiology* **586**, 3871–3879 (2008).

114. Zhang, S. Y., Jeffers, M. S., Lagace, D. C., Kirton, A. & Silasi, G. Developmental and Interventional Plasticity of Motor Maps after Perinatal Stroke. *J Neurosci* **41**, 6157–6172 (2021).

115. Silasi, G., Boyd, J. D., LeDue, J. & Murphy, T. H. Improved methods for chronic light-based motor mapping in mice: Automated movement tracking with accelerometers, and chronic EEG recording in a bilateral thin-skull preparation. *Front Neural Circuits* **0**, 123 (2013).

116. Hawkley, T. F., Preston, M. & Maani, C. V. Isoflurane. *xPharm: The Comprehensive Pharmacology Reference* 1–4 (2023) doi:10.1016/B978-008055232-3.61958-0.

117. Ishikawa, A. *et al.* The mechanism behind the inhibitory effect of isoflurane on angiotensin II-induced vascular contraction is different from that of sevoflurane. *Anesth Analg* **105**, 97–102 (2007).

118. Feng, G. *et al.* Imaging Neuronal Subsets in Transgenic Mice Expressing Multiple Spectral Variants of GFP. *Neuron* **28**, 41–51 (2000).

119. Zhao, S. *et al.* Cell type–specific channelrhodopsin-2 transgenic mice for optogenetic dissection of neural circuitry function. *Nature Methods 2011 8:9* **8**, 745–752 (2011).

120. Fenno, L. E., Gunaydin, L. A. & Deisseroth, K. Mapping Anatomy to Behavior in Thy1:18 ChR2-YFP Transgenic Mice Using Optogenetics. *Cold Spring Harb Protoc* **2015**, pdb.prot075598 (2015).

121. Nolan, M., Scott, C., Hof, P. R. & Ansorge, O. Betz cells of the primary motor cortex. *Journal of Comparative Neurology* vol. 532 1–29 Preprint at https://doi.org/10.1002/cne.25567 (2024).

122. Neafsey, E. J. *et al.* The organization of the rat motor cortex: A microstimulation mapping study. *Brain Res Rev* **11**, 77–96 (1986).

123. Luca, C. De. Electromyography. *Encyclopedia of Medical Devices and Instrumentation* (2006) doi:10.1002/0471732877.EMD097.

124. Peixoto, H. M., Cruz, R. M. S., Moulin, T. C. & Leão, R. N. Modeling the Effect of Temperature on Membrane Response of Light Stimulation in Optogenetically-Targeted Neurons. *Front Comput Neurosci* **14**, 479320 (2020).

125. Gysbrechts, B. *et al.* Light distribution and thermal effects in the rat brain under optogenetic stimulation. *J Biophotonics* **9**, 576–585 (2016).

126. Arias-Gil, G., Ohl, F. W., Takagaki, K. & Lippert, M. T. Measurement, modeling, and prediction of temperature rise due to optogenetic brain stimulation. *https://doi.org/10.1117/1.NPh.3.4.045007* **3**, 045007 (2016).

127. Papazoglou, A. *et al.* Non-restraining EEG Radiotelemetry: Epidural and Deep Intracerebral Stereotaxic EEG Electrode Placement. *J Vis Exp* **2016**, 54216 (2016).

128. Wang, X., Pinto-Duarte, A., Margarita Behrens, M., Zhou, X. & Sejnowski, T. J. Characterization of spatio-temporal epidural event-related potentials for mouse models of psychiatric disorders. *Scientific Reports 2015 5:1* **5**, 1–10 (2015).

129. Mégevand, P., Quairiaux, C., Lascano, A. M., Kiss, J. Z. & Michel, C. M. A mouse model for studying large-scale neuronal networks using EEG mapping techniques. *Neuroimage* **42**, 591–602 (2008).

130. Bai, Z., Zhang, J. & Fong, K. N. K. Intermittent Theta Burst Stimulation to the Primary Motor Cortex Reduces Cortical Inhibition: A TMS-EEG Study. *Brain Sciences 2021, Vol. 11, Page 1114* **11**, 1114 (2021).

131. Pellegrino, G. *et al.* Assessing cortical excitability with electroencephalography: A pilot study with EEG-iTBS. *Brain Stimul* **17**, 176–183 (2024).

132. Ding, Q. *et al.* Intermittent Theta Burst Stimulation Increases Natural Oscillatory Frequency in Ipsilesional Motor Cortex Post-Stroke: A Transcranial Magnetic Stimulation and Electroencephalography Study. *Front Aging Neurosci* **14**, 818340 (2022).

133. Rossini, P. M. & Rossi, S. Transcranial magnetic stimulation: Diagnostic, therapeutic, and research potential. *Neurology* **68**, 484–488 (2007).

134. A Clinical Guide to Transcranial Magnetic Stimulation - Google Books. https://books.google.ca/books?hl=en&lr=&id=8NnQAgAAQBAJ&oi=fnd&pg=PA152&dq=limitations+of+TMS&ots=A-ZkZ1tcKu&sig=FDWX4bhCNKlYOhlXmBbk0CF9gjQ#v=onepage&q=limitations%20of%20TMS&f=false.

135. Deriu, F. *et al.* Reporting quality of TMS studies in neurological conditions: A critical appraisal of the main gaps, challenges and clinical implications. *J Neurosci Methods* **362**, 109293 (2021).